Opioid use does not limit potent low-dose HIV-1 latency reversal agent boosting

Tyler Lilie[1]†, Jennifer Bouzy[1]†, Archana Asundi[2], Jessica Taylor[2,3], Samantha Roche[2], Alex Olson[2], Kendyll Coxen[1], Heather Corry[1], Hannah Jordan[1], Kiera Clayton[4], Nina Lin[2]‡, Athe Tsibris[1,5]‡*

† These authors contributed equally to this work

‡ These authors contributed equally to this work

Affiliations:

[1]Brigham and Women's Hospital, Boston, MA, USA.

[2]Department of Medicine, Boston University School of Medicine & Boston Medical Center, Boston, MA USA.

[3]Grayken Center for Addiction, Boston Medical Center, Boston, MA USA.

[4]Department of Pathology, University of Massachusetts T.H. Chan School of Medicine, Worcester, MA, USA.

[5]Harvard Medical School, Boston, MA, USA.

*Corresponding author: atsibris@bwh.harvard.edu

Abstract

The combined effects of the HIV-1 and opioid epidemics on virus reservoir dynamics are less well characterized. To assess the impact of opioid use on HIV-1 latency reversal, we studied forty-seven suppressed participants with HIV-1 and observed that lower concentrations of combination latency reversal agents (LRA) led to synergistic virus reactivation *ex vivo*, regardless of opioid use. The use of a Smac mimetic or low-dose protein kinase C agonist, compounds that did not reverse latency alone, in combination with low-dose histone deacetylase inhibitors generated significantly more HIV-1 transcription than phorbol 12-myristate 13-acetate (PMA) with ionomycin, the maximal known HIV-1 reactivator. This LRA boosting did not differ by sex or race and associated with greater histone acetylation in $CD4^+$ T cells and modulation of T cell phenotype. Virion production and the frequency of multiply spliced HIV-1 transcripts did not increase, suggesting a post-transcriptional block still limits potent HIV-1 LRA boosting.

Introduction

HIV-1 proviral DNA remains integrated in $CD4^+$ T cells during suppressive antiretroviral therapy (ART) and is a barrier to cure. This virus reservoir is seeded within days of infection before symptoms develop[1,2], persists[3-5], decays slowly[6], and can be maintained indefinitely[7,8]. The best approach to pursue HIV eradication remains uncertain. One strategy aims to pharmacologically reactivate latent HIV transcription in the setting of suppressive ART, induce virus protein production in infected cells, and then clear the reservoir, defined as cells that contain provirus capable of generating infectious virions, through immune-mediated mechanisms[9-11]. HIV-1 latency reversal agents (LRA) have advanced into clinical trials as monotherapy but with modest results; transient increases in virus mRNA production may be observed with some LRA but does not result in a decrease in reservoir size[12-22]. HIV-1 latency may be characterized by transcriptional blocks that cannot be overcome by single LRA[23-26].

To address these limitations, novel classes and combinations of LRA have been studied[27]. Epigenetic LRA such as histone deacetylase inhibitors, when combined with protein kinase C agonists or second mitochondria-derived activator of caspase (Smac) mimetics, have been reported under some conditions to synergistically increase HIV-1 transcription in $CD4^+$ T cells isolated from treated suppressed participants with HIV, although the precise mechanism for this synergy is unknown[28-32]. The absolute amount of HIV-1 latency reversal, defined most commonly as induced levels of HIV-1 cell-associated RNA (caRNA), reported with combination LRA is significantly less than that observed with the maximal HIV-1 reactivator, phorbol 12-myristate 13-acetate (PMA) and ionomycin. The effects of combination LRA on multiple splicing of HIV-1 RNA has been less well studied. A trade-off may exist between maximum synergy and maximum efficacy in combination LRA approaches[33].

People with HIV may be exposed to opioids, whether prescribed for chronic pain[34], prescribed for opioid use disorder[35], or injected as heroin[36] and have nearly double the risk of overdose compared to uninfected people who use opioids[37]. The pharmacology of opioids associated with substance use disorders may differ from opioid medications used to treat chronic pain. The μ opioid agonists, e.g. heroin, fentanyl, and methadone, can block IL-2 mRNA and protein production in activated T cells through inhibition of AP-1, NFAT, and NF-κB activation, transcription factors known to be positive regulators of HIV transcription initiation [38-40]. The effects of buprenorphine, a partial μ opioid agonist and κ and δ opioid antagonist used in the treatment of opioid use disorder, on HIV-1 latency and its reversal have not been explored. A recent finding suggested that people with HIV who use opioids may have diminished responses to latency reversal[41]; LRA efficacy in this burgeoning patient population is understudied.

To investigate the mechanisms that control HIV-1 latency reversal during opioid use, we enrolled a cohort of thirty-six treated, virologically suppressed participants with HIV. We tested LRA combinations at concentrations lower than those typically assessed and identified the phenomenon of LRA boosting: synergistic HIV-1 transcriptional reactivation with small molecules that do not reverse latency as single agents. We corroborated these findings in an additional eleven participants from a separate cohort without opioid use and identified key associations between potent LRA boosting, increases in histone acetylation, modulation of T cell phenotype and function, and downstream blocks in HIV-1 virion production. Importantly, we find that opioid use did not limit the magnitude or mechanisms of LRA boosting.

Results

Opioid use does not affect HIV-1 reservoir size

We enrolled a cohort from a single academic center of thirty-six treated suppressed participants with HIV who used, or did not use, opioids in a 2:1 ratio. Participants had a median age of 59 years, included one-third women, and were approximately 30% white (**Table 1**). The average duration of antiretroviral therapy was 12 years with a median duration of undetectable plasma HIV-1 RNA levels of over six years. Participant characteristics were further defined by type of opioid use (**Suppl. Table 1**) and validated by urine toxicology and self-reported substance use questionnaires (**Suppl. Fig. 1**). This cohort comprised participants who actively injected opioids (n=4), used methadone (n=4) or suboxone (n=12) as medication for opioid use disorder, or took opioids for chronic pain (n=4). Amphetamine and barbiturate use was not detected. All active injection opioid users had confirmatory urine toxicology screens positive for fentanyl (n=2 of 4, range 62 - >500 ng/mL) and/or norfentanyl (n=4 of 4 participants, range 46 - >500 ng/mL) and reported a median of 6 days of injection opioid use in the preceding 30 days (IQR 4-16 days) with a median of 7 days since the most recent use (IQR 4-14 days). All participants in the methadone, buprenorphine, and prescription opioid subgroups had urine toxicology positive for that substance.

To assess markers of HIV-1 persistence, we quantified total HIV-1 DNA and caRNA in PBMC and evaluated intact proviral reservoir size. Total HIV-1 DNA levels were similar between opioid and non-opioid groups, 2.36 vs 2.38 $\log_{10}$ copies/10^6 PBMC, respectively, as were HIV-1 caRNA levels, 2.45 vs 2.52 $\log_{10}$ copies/10^6 PBMC (**Fig. 1a**). Levels of intact provirus DNA were also similar between groups, 2.00 vs 1.82 $\log_{10}$ copies/10^6 PBMC. To better define the intact proviral DNA reservoir, we characterized 5' and 3' HIV-1 deletions across

cohorts and opioid use subgroups (**Fig. 1b-c**). Similar proportions of intact 5' and 3' genetic regions were observed, irrespective of opioid use. The ratios of proviruses containing an intact 5' region and a defective (hypermutated) or deleted 3' region in HIV-1 *env* were statistically similar. An exploratory analysis demonstrated a greater proportion of total genomes were intact in active opioid users (**Fig. 1d**).

LRA boosting markedly increases HIV-1 transcription

To determine the effects of opioid use on HIV-1 latency reversal *ex vivo*, we isolated PBMC from all OPHION participants and tested a panel of ten LRA conditions (**Fig. 2**). The histone deacetylase inhibitors (HDACi) romidepsin (RMD) and panobinostat (PNB) were used at the lowest concentrations most commonly reported in the literature and the protein kinase C agonist bryostatin was tested at 1nM, one-tenth the most commonly reported concentration. In single LRA conditions, we observed a 2.7-fold activation of HIV-1 caRNA transcription, relative to an untreated DMSO-containing control, with αCD3/αCD28 beads (95% CI [2.2, 3.2]), a T cell receptor (TCR) agonist (**Fig. 2a**). Greater reactivation was observed with RMD (3.8-fold increase, 95% CI [3.2, 4.3]) when compared to PNB (2.6-fold increase, 95% CI [2.2, 3.0]). Low-dose bryostatin minimally increased unspliced HIV-1 caRNA levels (1.2-fold increase, 95% CI [1.1, 1.4]), but the Smac mimetic AZD5582, at a standard concentration[42], did not (0.9-fold increase, 95% CI [0.8, 1.1]).

We next assessed LRA in combination. Incubation of PBMC with HDACi and either AZD5582 (AZD) or low-dose bryostatin potentiated HIV-1 latency reversal. AZD in combination with PNB or RMD increased HIV-1 caRNA levels 8.1-fold (95% CI [6.5, 9.2]) and 9.1-fold (95% CI [7.4, 10.8]), respectively. Low-dose bryostatin with PNB increased HIV-1

caRNA 10.6-fold (95% CI [8.9, 12.2]), whereas the greatest fold-induction of HIV-1 caRNA was observed with the combination of low-dose bryostatin and RMD (13.2-fold, 95% CI [11.2, 15.2]). Statistically greater HIV-1 RNA induction was observed with the LRA boosting combinations relative to HDACi monotherapy and TCR agonism, when corrected for multiple comparisons. We compared LRA response as a function of opioid use (**Fig. 2b**), sex (**Fig. 2c**), race (**Fig. 2d**), and ethnicity (**Suppl. Fig. 2**) and observed no statistically significant differences in the fold-changes of HIV-1 caRNA induction across these groups. In an exploratory analysis, the fold-change in HIV-1 caRNA varied by opioid use subgroup in response to T cell receptor agonism (**Fig. 2e**). Statistically significantly greater reactivation was observed in the suboxone sub-group when compared to active injection opioid users, the group with the smallest fold-change in αCD3/αCD28 bead-induced HIV-1 caRNA levels.

LRA boosting modulates T cell activation and cytokine production

To understand whether LRA exposure activates $CD4^+$ T cells, we assessed the upregulation of surface activation-induced markers (AIM) [43]. We leveraged dual-marker AIM assays (**Suppl. Fig. 3, Fig. 3a**), originally developed to detect T cell antigen responsiveness, to quantify cellular activation that occurs with LRA exposure, outside the context of peptide-specific recognition. Using TCR agonism as a positive control, responses were detected in 49% (95% CI [45, 54]), 32% (95% CI [28, 35]), and 42% (95% CI [36, 47]) of $CD4^+$ T cells in the OX40/PDL1, OX40/CD25, and CD69/CD40L AIM assays, respectively (**Fig. 3b**). Low-dose bryostatin significantly upregulated surface expression to more modest levels in all three AIM assays, relative to an untreated control condition. Bryostatin induced OX40/PDL1 surface expression in 5.2% of $CD4^+$ T cells (95% CI [3,4, 7.0]), levels of induction that did not

significantly change when used in combination with RMD (5.4%, 95% CI [3.3, 7.4]) or PNB (3.5%, 95% CI [2.1, 5.0]). Bryostatin monotherapy induced expression in 6.9% (95% CI [5.6, 8.3]) and 2.6% (95% CI [2.0, 3.2]) of CD4s in the OX40/CD25 and CD69/CD40L AIM assays, respectively. In these two assays, the combination of RMD or PNB with low-dose bryostatin reduced activation-induced markers, relative to bryostatin alone, in some cases to undetectable levels; these findings did not differ by opioid use. The remainder of the LRA panel and their combinations did not upregulate surface expression in any AIM assay (**Suppl. Fig. 4a-c)**.

We observed a more pronounced upregulation in isolated CD69 expression, an early activation marker, in response to LRA (**Fig. 3c**). Approximately 0.5% (95% CI [0.4, 0.7]) of untreated $CD4^+$ T cells expressed CD69 after 18 hours in culture. The proportion of cells expressing surface CD69 significantly increased to similar levels with TCR agonism (68.5%, 95% CI [63.1, 73.9]) and low-dose bryostatin (72.9%, 95% CI [69.2, 76.5]). Whereas AZD5582 (1.0%, 95% CI [0.7, 1.2]), RMD (4.7%, 95% CI [3.1, 6.3]), and PNB (5.4%, 95% CI [3.8, 7.0]) modestly increased CD69 levels, combinations of these small molecules led to synergistic effects. Significantly greater induction of CD69 expression was observed when RMD or PNB was combined with bryostatin or AZD5582; a bryostatin combination induced more CD69 than an HDACi plus AZD5582. CD69 levels were statistically similar when comparing TCR agonism, bryostatin alone, and bryostatin in combination with either HDACi (**Suppl. Fig. 4d**).

To further assess LRA effects on T cell activation, we stained $CD4^+$ and $CD8^+$ T cells for intracellular cytokine production (**Fig. 3d-e**). We observed a cytokine production hierarchy in CD4s, where TNF-α > IL-2 > IFN-γ, and in CD8s, where TNF-α > IFN-γ > IL-2. In response to TCR agonism, significantly more $CD4^+$ T cells (CD4s) produce TNF-α (30.4%, 95% CI [27.5, 33.4]) than IL-2 (14.3%, 95% CI [12.5, 16.1]) or IFN-γ (6.0%, 95% CI [4.9, 7.1]), and

significantly more IL-2 than IFN-γ (**Suppl. Fig. 4e**). We identified a different hierarchy in $CD8^+$ T cells (CD8s), where the proportion of cells producing TNF-α remained greatest (17.5%, 95% CI [13.9, 21.1]) but significantly more IFN-γ (9.0%, 95% CI [7.1, 10.9]) was produced than IL-2 (4.3%, 95% CI [2.8, 5.9]). Whereas HDACi monotherapy did not increase the proportion of CD4s or CD8s producing cytokines compared to an untreated control, low-dose bryostatin alone or in combination with HDACi significantly increased production of TNF-α and, to a smaller magnitude, IFN-γ in CD4s. Significantly more CD4s produced TNF-α than IFN-γ in response to RMD + bryostatin (4.5%, 95% CI [3.5, 5.6] versus 1.3%, 95% CI [0.9, 1.7]) and PNB + bryostatin (4.2%, 95% CI [3.4, 5.0] versus 1.7%, 95% CI [1.0, 2.4]). In CD8s, low-dose bryostatin significantly increased production of TNF-α (2.8%, 95% CI [1.9, 3.8]) and IFN-γ (1.5%, 95% CI [0.9, 2.0]). The proportions of CD8s that produced TNF-α and IFN-γ when exposed to the combinations of RMD + bryostatin (3.4%, 95% CI [2.5, 4.4] versus 4.7%, 95% CI [2.8, 6.6]) and PNB + bryostatin (4.1%, 95% CI [2.9, 5.3] versus 4.6%, 95% CI [3.0, 6.3]) were similar. IL-2 production did not increase above 0.1% of CD4s or CD8s for any LRA, or combination, we tested. Cytokine production did not differ by opioid use (**Suppl. Fig. 5**).

LRA boosting increases histone acetylation

To investigate the mechanism(s) of LRA boosting, we next assessed histone acetylation. The proportions of acetylated histone $H3^+$ live CD4s were similar between untreated cells (19.7%, 95% CI [16.9, 22.4]) and cells exposed to RMD (21.8%, 95% CI [19.4, 24.3]), PNB (21.7%, 95% CI [19.3, 24.2]), or AZD (19.8%, 95% CI [17.1, 22.6]) and significantly increased after single-LRA exposure to αCD3/αCD28 beads (35.5%, 95% CI [32.7, 38.4]) and low-dose bryostatin (29.2%, 95% CI [25.7, 32.6]) (**Fig. 4a**). Low-dose bryostatin in combination with

206 either RMD (36.8%, 95% CI [32.1, 43.2]) or PNB (37.5%, 95% CI [31.8, 43.2]) significantly
207 increased the proportions of CD4s contained acetylated histone H3. Interestingly, statistically
208 significant increases in acetylated histone $H3^+$ live CD4s were also observed when combining
209 LRA which individually did not affect acetylation, specifically RMD + AZD (30.0%, 95% CI
210 [26.9, 33.1]) and PNB + AZD (29.8%, 95% CI [26.5, 33.0]). These results did not differ by
211 opioid use (**Suppl. Fig 6a**).

212 Levels of acetylated histone H3, measured by median fluorescence intensity (MFI), were
213 similar in untreated live CD4s and in cells cultured with αCD3/αCD28 beads, low-dose
214 bryostatin, or AZD (**Fig. 4b**). Significant 3.4-fold and 3.3-fold increases in acetyl histone MFI
215 were observed for RMD (21482, 95% CI [19014, 23951]) and PNB (21070, 95% CI [18727,
216 23413]), respectively. AZD in combination with RMD or PNB further increased MFI by 6.1-
217 fold and 5.7-fold, respectively. Absolute increases in MFI were observed for low-dose bryostatin
218 in combination with RMD (25498, 95% CI [22772, 28225]) or PNB (27651, 95% CI [24729,
219 30573]) but did not retain significance after correction for multiple comparisons. These results
220 did not differ by opioid use (**Suppl. Fig 6b**). We observed no association between acetylated
221 histone H3 MFI and fold-change in HIV-1 RNA levels for HDACi monotherapy or for HDACi
222 in combination with AZD (**Fig 4c-d**). A statistically significant weak association between the
223 proportion of acetyl histone $H3^+$ CD4s and fold-change in HIV-1 RNA levels was detected for
224 HDACi in combination with bryostatin (**Fig 4e**).

225

226 **LRA boosting does not consistently induce virion production**

227 To extend our analyses from the OPHION cohort, we studied an additional eleven
228 participants with HIV who did not use opioids, enrolled in the HEAL cohort (**Suppl. Table 2**).

We compared LRA boosting responses to the most potent known HIV-1 LRA, PMA in combination with ionomycin (PMA-iono). Significant fold-change increases in HIV-1 transcription were observed with combinations of low-dose bryostatin with RMD (8.3-fold, 95% CI [7.2, 9.5]) or PNB (8.0-fold, 95% CI [6.9, 9.0]), when compared to RMD alone (3.4-fold, 95% CI [2.6, 4.2]), PNB alone (3.1-fold, 95% CI [2.6, 3.6]), or PMA-iono (1.6-fold, 95% CI [1.4, 1.9]) (**Fig. 5a**). In separate experiments, we did not observe statistically greater HIV-1 transcription with an HDACi in combination with AZD, relative to PMA-iono, in contrast to the results from the larger OPHION cohort (**Fig 5b**). No significant increases in HIV-1 transcription were observed in PBMC experiments with low-dose bryostatin (1.0-fold, 95% CI 0.9 – 1.1) or AZD (1.2-fold, 95% CI 0.6 – 1.9). Similar magnitudes of HIV-1 transcriptional reactivation were seen with HDACi monotherapy, low-dose bryostatin, and AZD monotherapy across the OPHION and HEAL cohorts we studied. We evaluated human reference gene transcription during LRA treatment and observed decreases with HDACi exposure, increases with PMA-iono, and variable changes with bryostatin (**Suppl. Fig. 7**).[44,45]

To assess the magnitude of HIV-1 latency reversal as a function of cell type, we next performed parallel experiments in PBMC and total $CD4^+$ T cells (**Fig. 5c**). Levels of HIV-1 caRNA were, on average, 4.3-fold higher (range 3.2 – 6.0) across experimental conditions performed in $CD4^+$ T cells, when compared to PBMC, and varied by 1.6 $\log_{10}$ (PBMC) and 1.8 $\log_{10}$ (CD4) across participant samples in the absence of LRA. To control for absolute caRNA differences, we determined fold-changes in LRA response and observed statistically significant increases in HIV-1 caRNA with low-dose bryostatin in combination with RMD or PNB, when compared to PMA-iono, in both PBMC and CD4s (**Fig. 5d**). To explore the variance in LRA response, we compiled per-participant biological replicate measurements (**Suppl. Fig. 8a**).

Supernatant HIV-1 RNA levels increased after 24hr incubation of PBMC with PMA-iono (19 copies/mL, 95% CI [10, 32]) and the combinations of RMD plus bryostatin (27 copies/mL, 95% CI [11, 34]) or AZD (31 copies/mL, 95% CI [14, 43]), and PNB plus bryostatin (35 copies/mL, 95% CI [19, 60]) or AZD (12 copies/mL, 95% CI [8.1, 26]), when compared to untreated PBMC (3.0 copies/mL, 95% CI [2.2, 6.9]), but these results were not statistically significant after correction for multiple comparisons (**Fig. 5e**). This virion production response was biphasic. For each LRA condition, PBMC samples from at least 5 of 10 participants showed no increases in HIV-1 RNA levels over control; these were most commonly the same participants. Additionally, no significant increases in LRA-induced virion production in $CD4^+$ T cell cultures were observed. Notably, greater virion production in untreated CD4s and greater absolute magnitudes of supernatant viremia in LRA treated CD4s were noted, relative to PBMC, but were again driven by increases from a subset of participants. To investigate the nature of this post-transcriptional block more precisely, we quantified the frequency of CD4s with inducible multiply spliced HIV-1 RNA transcripts (**Fig. 5f**) [46]. No significant increases in HIV-1 *tat*/*rev* transcripts were observed with RMD in combination with bryostatin at either 1nM or 10nM concentrations. In a post-hoc analysis, we combined datasets from OPHION and HEAL participants, including LRA conditions common to both sets of experiments, and observed statistically significant increases in HIV-1 unspliced RNA transcription with all LRA boosting combinations (**Fig. 5g**). The variance in LRA responseincreased as the magnitude of fold change in HIV-1 caRNA increased (**Suppl. Fig 8b**).

Discussion

Opioid use is complex and can be accompanied by comorbidities, such as immune activation with injection drug use [47,48], that may impact the HIV-1 reservoir and its persistence [45,49-52]. Here, we found no effects of opioid use by indication, type, or pharmacology on markers of HIV-1 persistence. In the setting of persistently suppressed viremia, opioid use was less likely to modulate virus reservoir size. While our OPHION study participants were older than opioid users experiencing the greatest number of overdose deaths [53], they do reflect an age more typical for patients with HIV who engage in research locally. Overall, participants were matched on the duration of ART and the duration of virus suppression, key variables that have been associated with HIV-1 reservoir size, [54] and our urine toxicology results were consistent with the participants' ascribed opioid use group. We found that opioid use generally did not impact LRA responsiveness, in contrast to a recent smaller study [41]. Our relatively large sample size allowed us to determine that this potency was less likely to be affected by sex, race, or ethnicity.

We used these samples to identify and characterize the phenomenon of LRA boosting: improving the potency of HDACi beyond that of PMA-ionomycin by combining with a 2nd drug that does not, by itself, re-activate HIV-1 transcription. This boosting occurred at lower LRA concentrations, here at least half the RMD and 1/10th the bryostatin concentrations used in prior combination studies [28-31]. The specific synergistic latency reversal effects of low-dose bryostatin and romidepsin was previously identified in samples from four participants with HIV [28]. Here we confirm those findings in a larger sample size and extend the observation to HDACi more generally. While AZD5582 monotherapy induced virus transcription in tissues from animal models, we observed no HIV-1 latency reversal, at an identical dose, in PBMC isolated from the 47 participants we tested [42]. We observed greater *ex vivo* LRA efficacy of HDACi monotherapy,

298 relative to AZD5582. In this regard, our findings agree with a recent study that assessed a higher
299 AZD5582 concentration, although this study did not identify HDACi-AZD synergy, relative to
300 HDACi monotherapy, using higher LRA concentrations [32]. Interestingly, the fold-change in
301 HIV-1 RNA levels that we observed with PMA-ionomycin were orders of magnitude lower than
302 some prior studies [28,32]. Here, we calculated levels of HIV-1 caRNA copy number in response to
303 LRA on a per-cell basis, rather than the induction of HIV-1 transcripts on a weight basis, per μg
304 of RNA. These differences did not appear to be a function of the cell type used for latency
305 reversal, PBMC versus total $CD4^+$ T cells, and it remains unclear if assay technicalities or
306 quantification methodology may contribute.

307 The use of two HDACi in our panel of ten LRA conditions increased the generalizability
308 of the findings we observed with this drug class. Similar magnitudes of boosting were observed
309 with RMD and PNB and suggests that class I histone deacetylase inhibition may be more
310 relevant to this phenomenon [55]. LRA boosting correlated with increased histone H3 acetylation
311 in $CD4^+$ T cells but AZD-associated boosting did not recruit additional CD4s with acetylated
312 histone H3. HDACi monotherapy also did not increase the proportions of acetylated histone H3-
313 positive CD4s and the amount of acetylated histone H3 per cell did not meaningfully correlate
314 with the induction of HIV-1 transcription. It remains unclear if histone acetylation is correlative
315 or causative to virus reactivation. In the context of cellular genes, histone acetylation is not an
316 immediate driver of the transcriptional changes observed with HDACi [56]. Similar magnitudes of
317 HIV-1 reactivation were observed with low-dose bryostatin- and AZD5582-mediated HDACi
318 boosting and could share common mechanisms. Bryostatin and AZD5582 can activate canonical
319 and non-canonical NF-κB pathways, respectively, and the overlap in signaling with LRA
320 boosting requires further definition.

LRA boosting, and their individual components, can have off-target effects. Whereas CD69 surface expression has been proposed as a biomarker of latency reversal potency in the context of PKC agonists, we found no correlation between CD69 upregulation and the magnitude of latency reversal [57]. Low-dose bryostatin was sufficient to increase surface activation-induced markers and increase cytokine production in $CD4^+$ and $CD8^+$ T cells, albeit to relatively low levels, either alone or in combination with HDACi. Our results confirm and extend previous findings on the effects of combination LRA on T lymphocytes [58]. In contrast, LRA boosting with AZD5582 resulted in relatively lower surface levels of CD69 and no induction of surface activation markers or cytokine production in T cells. An LRA boosting approach that minimizes immune modulatory effects may be more appealing as an investigational intervention.

The variance in HIV-1 LRA responsiveness we document, across participants and replicates, has implications for future studies. Small studies may be limited in their capacity to accurately quantify this variability, which increases with LRA potency. Assessments of LRA activity should prioritize larger sample sizes and more than one biological replicate per participant. We found that normalization of HIV-1 transcription to host gene transcription may introduce additional variability. Despite HIV-1 re-activation that was superior to PMA-ionomycin, multiply spliced HIV-1 transcription and virion production did not increase with LRA boosting. Blocks to HIV-1 splicing are increasingly recognized, and here we extend those findings to novel LRA boosting combinations [23-25,59-61]. Future work must focus on the post-transcriptional mechanisms of HIV-1 RNA processing and inter-patient differences in LRA responsiveness, which facilitate virion production during TCR agonism and treatment with PMA-ionomycin and which may not be active during HIV-1 latency or LRA boosting.

Our study has limitations. Prior and current injection opioid use limits the peripheral blood draw volumes we could obtain; this required us to prioritize experiments with a given sample. The statistical significance of LRA boosting with AZD5582-containing regimens was not replicated in our HEAL cohort samples and it is unclear if this relates to the variability in LRA response as sample size decreases or to unrecognized differences between our cohort's participants. Additional mechanisms are likely to explain how LRA boosting increases virus transcription. Bryostatin may exert its HIV-1 latency reversal effects independently of PKC agonism [62].

The use of HIV-1 LRA at sub-maximal doses and in combination with small molecules that do not increase virus transcription, *ex vivo*, expands our understanding of how virus latency may be reversed. Follow-on studies should delineate the precise mechanisms required for efficient virus RNA processing and virion production and identify new discovery targets for future development.

Acknowledgements

This work is supported by the National Institutes of Health (NIH) R61 DA047038 (NL and AT) and R33 DA047038 (AT) and was facilitated by the Providence/Boston Center for AIDS Research (P30AI042853) and the Harvard University Center for AIDS Research (P30AI060354). The project described was further supported by Clinical Translational Science Award 1UL1TR002541-01 to Harvard University and Brigham and Women's Hospital from the National Center for Research Resources. The content is solely the responsibility of the authors and does not necessarily represent the official views of the National Center for Research Resources or the National Institutes of Health.

References

1. Chun, T.W., *et al.* Early establishment of a pool of latently infected, resting CD4(+) T cells during primary HIV-1 infection. *Proceedings of the National Academy of Sciences of the United States of America* **95**, 8869-8873 (1998).
2. Whitney, J.B., *et al.* Rapid seeding of the viral reservoir prior to SIV viraemia in rhesus monkeys. *Nature* **512**, 74-77 (2014).
3. Wong, J.K., *et al.* Recovery of replication-competent HIV despite prolonged suppression of plasma viremia. *Science (New York, N.Y* **278**, 1291-1295 (1997).
4. Chun, T.W., *et al.* Presence of an inducible HIV-1 latent reservoir during highly active antiretroviral therapy. *Proceedings of the National Academy of Sciences of the United States of America* **94**, 13193-13197 (1997).
5. Finzi, D., *et al.* Latent infection of CD4+ T cells provides a mechanism for lifelong persistence of HIV-1, even in patients on effective combination therapy. *Nature medicine* **5**, 512-517 (1999).
6. Siliciano, J.D., *et al.* Long-term follow-up studies confirm the stability of the latent reservoir for HIV-1 in resting CD4+ T cells. *Nature medicine* **9**, 727-728 (2003).
7. Chomont, N., *et al.* HIV reservoir size and persistence are driven by T cell survival and homeostatic proliferation. *Nature medicine* **15**, 893-900 (2009).
8. Mullins, J.I. & Frenkel, L.M. Clonal Expansion of Human Immunodeficiency Virus-Infected Cells and Human Immunodeficiency Virus Persistence During Antiretroviral Therapy. *The Journal of infectious diseases* **215**, S119-S127 (2017).
9. Deeks, S.G., *et al.* International AIDS Society global scientific strategy: towards an HIV cure 2016. *Nature medicine* (2016).

10. Ferrari, G., Pollara, J., Tomaras, G.D. & Haynes, B.F. Humoral and Innate Antiviral Immunity as Tools to Clear Persistent HIV Infection. *The Journal of infectious diseases* **215**, S152-S159 (2017).

11. Riley, J.L. & Montaner, L.J. Cell-Mediated Immunity to Target the Persistent Human Immunodeficiency Virus Reservoir. *The Journal of infectious diseases* **215**, S160-S171 (2017).

12. McMahon, D.K.*, et al.* A Phase 1/2 Randomized, Placebo-Controlled Trial of Romidespin in Persons With HIV-1 on Suppressive Antiretroviral Therapy. *The Journal of infectious diseases* **224**, 648-656 (2021).

13. Scully, E.P.*, et al.* Impact of Tamoxifen on Vorinostat-Induced Human Immunodeficiency Virus Expression in Women on Antiretroviral Therapy: AIDS Clinical Trials Group A5366, The MOXIE Trial. *Clin Infect Dis* **75**, 1389-1396 (2022).

14. Gutierrez, C.*, et al.* Bryostatin-1 for latent virus reactivation in HIV-infected patients on antiretroviral therapy. *AIDS (London, England)* **30**, 1385-1392 (2016).

15. Archin, N.M.*, et al.* HIV-1 expression within resting CD4+ T cells after multiple doses of vorinostat. *The Journal of infectious diseases* **210**, 728-735 (2014).

16. Archin, N.M.*, et al.* Administration of vorinostat disrupts HIV-1 latency in patients on antiretroviral therapy. *Nature* **487**, 482-485 (2012).

17. Elliott, J.H.*, et al.* Activation of HIV transcription with short-course vorinostat in HIV-infected patients on suppressive antiretroviral therapy. *PLoS pathogens* **10**, e1004473 (2014).

18. Sogaard, O.S.*, et al.* The Depsipeptide Romidepsin Reverses HIV-1 Latency In Vivo. *PLoS pathogens* **11**, e1005142 (2015).

19. Rasmussen, T.A., *et al.* Panobinostat, a histone deacetylase inhibitor, for latent-virus reactivation in HIV-infected patients on suppressive antiretroviral therapy: a phase 1/2, single group, clinical trial. *The lancet. HIV* **1**, e13-21 (2014).

20. Routy, J.P., *et al.* Valproic acid in association with highly active antiretroviral therapy for reducing systemic HIV-1 reservoirs: results from a multicentre randomized clinical study. *HIV medicine* **13**, 291-296 (2012).

21. Sagot-Lerolle, N., *et al.* Prolonged valproic acid treatment does not reduce the size of latent HIV reservoir. *AIDS (London, England)* **22**, 1125-1129 (2008).

22. Archin, N.M., *et al.* Interval dosing with the HDAC inhibitor vorinostat effectively reverses HIV latency. *The Journal of clinical investigation* **127**, 3126-3135 (2017).

23. Yukl, S.A., *et al.* HIV latency in isolated patient CD4(+) T cells may be due to blocks in HIV transcriptional elongation, completion, and splicing. *Science translational medicine* **10**(2018).

24. Moron-Lopez, S., *et al.* Characterization of the HIV-1 transcription profile after romidepsin administration in ART-suppressed individuals. *AIDS (London, England)* **33**, 425-431 (2019).

25. Zerbato, J.M., *et al.* Multiply spliced HIV RNA is a predictive measure of virus production ex vivo and in vivo following reversal of HIV latency. *EBioMedicine* **65**, 103241 (2021).

26. Martin, H.A., *et al.* New Assay Reveals Vast Excess of Defective over Intact HIV-1 Transcripts in Antiretroviral Therapy-Suppressed Individuals. *Journal of virology* **96**, e0160522 (2022).

27. Rodari, A., Darcis, G. & Van Lint, C.M. The Current Status of Latency Reversing Agents for HIV-1 Remission. *Annu Rev Virol* **8**, 491-514 (2021).

28. Laird, G.M., *et al.* Ex vivo analysis identifies effective HIV-1 latency-reversing drug combinations. *The Journal of clinical investigation* **125**, 1901-1912 (2015).

29. Pache, L., *et al.* BIRC2/cIAP1 Is a Negative Regulator of HIV-1 Transcription and Can Be Targeted by Smac Mimetics to Promote Reversal of Viral Latency. *Cell host & microbe* **18**, 345-353 (2015).

30. Grau-Exposito, J., *et al.* Latency reversal agents affect differently the latent reservoir present in distinct CD4+ T subpopulations. *PLoS pathogens* **15**, e1007991 (2019).

31. Pardons, M., Fromentin, R., Pagliuzza, A., Routy, J.P. & Chomont, N. Latency-Reversing Agents Induce Differential Responses in Distinct Memory CD4 T Cell Subsets in Individuals on Antiretroviral Therapy. *Cell Rep* **29**, 2783-2795 e2785 (2019).

32. Dai, W., *et al.* Genome-wide CRISPR screens identify combinations of candidate latency reversing agents for targeting the latent HIV-1 reservoir. *Science translational medicine* **14**, eabh3351 (2022).

33. Gupta, V. & Dixit, N.M. Trade-off between synergy and efficacy in combinations of HIV-1 latency-reversing agents. *PLoS computational biology* **14**, e1006004 (2018).

34. Edelman, E.J., *et al.* Receipt of opioid analgesics by HIV-infected and uninfected patients. *J Gen Intern Med* **28**, 82-90 (2013).

35. Reddon, H., *et al.* Methadone maintenance therapy decreases the rate of antiretroviral therapy discontinuation among HIV-positive illicit drug users. *AIDS Behav* **18**, 740-746 (2014).

456 36. Tavitian-Exley, I., Vickerman, P., Bastos, F.I. & Boily, M.C. Influence of different drugs
457 on HIV risk in people who inject: systematic review and meta-analysis. *Addiction* **110**,
458 572-584 (2015).
459 37. Green, T.C., McGowan, S.K., Yokell, M.A., Pouget, E.R. & Rich, J.D. HIV infection and
460 risk of overdose: a systematic review and meta-analysis. *AIDS (London, England)* **26**,
461 403-417 (2012).
462 38. Borner, C., Kraus, J., Bedini, A., Schraven, B. & Hollt, V. T-cell receptor/CD28-
463 mediated activation of human T lymphocytes induces expression of functional mu-opioid
464 receptors. *Mol Pharmacol* **74**, 496-504 (2008).
465 39. Borner, C.*, et al.* Mechanisms of opioid-mediated inhibition of human T cell receptor
466 signaling. *J Immunol* **183**, 882-889 (2009).
467 40. Mbonye, U. & Karn, J. Transcriptional control of HIV latency: Cellular signaling
468 pathways, epigenetics, happenstance and the hope for a cure. *Virology* (2014).
469 41. Basukala, B.*, et al.* Virally Suppressed People Living with HIV Who Use Opioids Have
470 Diminished Latency Reversal. *Viruses* **15**(2023).
471 42. Nixon, C.C.*, et al.* Systemic HIV and SIV latency reversal via non-canonical NF-kappaB
472 signalling in vivo. *Nature* **578**, 160-165 (2020).
473 43. Reiss, S.*, et al.* Comparative analysis of activation induced marker (AIM) assays for
474 sensitive identification of antigen-specific CD4 T cells. *PLoS ONE* **12**, e0186998 (2017).
475 44. Ceriani, C.*, et al.* Defining stable reference genes in HIV latency reversal experiments.
476 *Journal of virology* **95**(2021).

45. Gandhi, R.T., *et al.* Levels of HIV-1 persistence on antiretroviral therapy are not associated with markers of inflammation or activation. *PLoS pathogens* **13**, e1006285 (2017).

46. Procopio, F.A., *et al.* A Novel Assay to Measure the Magnitude of the Inducible Viral Reservoir in HIV-infected Individuals. *EBioMedicine* **2**, 874-883 (2015).

47. Mehandru, S., *et al.* Behavioural, Mucosal and Systemic Immune Parameters in HIV-infected and Uninfected Injection Drug Users. *J Addict Res Ther* **6**, 1-8 (2015).

48. Deren, S., Cleland, C.M., Lee, H., Mehandru, S. & Markowitz, M. Brief Report: The Relationship Between Injection Drug Use Risk Behaviors and Markers of Immune Activation. *Journal of acquired immune deficiency syndromes (1999)* **75**, e8-e12 (2017).

49. Khoury, G., *et al.* Human Immunodeficiency Virus Persistence and T-Cell Activation in Blood, Rectal, and Lymph Node Tissue in Human Immunodeficiency Virus-Infected Individuals Receiving Suppressive Antiretroviral Therapy. *The Journal of infectious diseases* **215**, 911-919 (2017).

50. Massanella, M., Fromentin, R. & Chomont, N. Residual inflammation and viral reservoirs: alliance against an HIV cure. *Current opinion in HIV and AIDS* **11**, 234-241 (2016).

51. Ruggiero, A., *et al.* During Stably Suppressive Antiretroviral Therapy Integrated HIV-1 DNA Load in Peripheral Blood is Associated with the Frequency of CD8 Cells Expressing HLA-DR/DP/DQ. *EBioMedicine* **2**, 1153-1159 (2015).

52. Cockerham, L.R., *et al.* CD4+ and CD8+ T cell activation are associated with HIV DNA in resting CD4+ T cells. *PLoS ONE* **9**, e110731 (2014).

499 53. Spencer, M.R., Minino, A.M. & Warner, M. Drug Overdose Deaths in the United States,
500 2001-2021. *NCHS Data Brief*, 1-8 (2022).
501 54. Bachmann, N.*, et al.* Determinants of HIV-1 reservoir size and long-term dynamics
502 during suppressive ART. *Nat Commun* **10**, 3193 (2019).
503 55. Milazzo, G.*, et al.* Histone Deacetylases (HDACs): Evolution, Specificity, Role in
504 Transcriptional Complexes, and Pharmacological Actionability. *Genes (Basel)* **11**(2020).
505 56. Halsall, J.A., Turan, N., Wiersma, M. & Turner, B.M. Cells adapt to the epigenomic
506 disruption caused by histone deacetylase inhibitors through a coordinated, chromatin-
507 mediated transcriptional response. *Epigenetics Chromatin* **8**, 29 (2015).
508 57. Marsden, M.D.*, et al.* In vivo activation of latent HIV with a synthetic bryostatin analog
509 effects both latent cell "kick" and "kill" in strategy for virus eradication. *PLoS pathogens*
510 **13**, e1006575 (2017).
511 58. Walker-Sperling, V.E., Pohlmeyer, C.W., Tarwater, P.M. & Blankson, J.N. The Effect of
512 Latency Reversal Agents on Primary CD8+ T Cells: Implications for Shock and Kill
513 Strategies for Human Immunodeficiency Virus Eradication. *EBioMedicine* **8**, 217-229
514 (2016).
515 59. Wedrychowski, A.*, et al.* Transcriptomic Signatures of Human Immunodeficiency Virus
516 Post-Treatment Control. *Journal of virology* **97**, e0125422 (2023).
517 60. Moron-Lopez, S.*, et al.* Human splice factors contribute to latent HIV infection in
518 primary cell models and blood CD4+ T cells from ART-treated individuals. *PLoS*
519 *pathogens* **16**, e1009060 (2020).

61. Mota, T.M., *et al.* Integrated Assessment of Viral Transcription, Antigen Presentation, and CD8(+) T Cell Function Reveals Multiple Limitations of Class I-Selective Histone Deacetylase Inhibitors during HIV-1 Latency Reversal. *Journal of virology* **94**(2020).

62. Mbonye, U., Leskov, K., Shukla, M., Valadkhan, S. & Karn, J. Biogenesis of P-TEFb in CD4+ T cells to reverse HIV latency is mediated by protein kinase C (PKC)-independent signaling pathways. *PLoS pathogens* **17**, e1009581 (2021).

63. McLellan, A.T., *et al.* The Fifth Edition of the Addiction Severity Index. *J Subst Abuse Treat* **9**, 199-213 (1992).

64. Institute of Behavioral Research. Texas Christian University Drug Screen 5. Fort Worth: Texas Christian University, Institute of Behavioral Research (2020) (https://ibr.tcu.edu/forms/tcu-drug-screen/).

65. Malnati, M.S., *et al.* A universal real-time PCR assay for the quantification of group-M HIV-1 proviral load. *Nature protocols* **3**, 1240-1248 (2008).

66. Bruner, K.M., *et al.* A quantitative approach for measuring the reservoir of latent HIV-1 proviruses. *Nature* **566**, 120-125 (2019).

Table 1. OPHION Participant Characteristics

Characteristic	Cohort		Total*
	Non-Opioid	Opioid	
Participants, N	12	24	36
Age			
Median (IQR†)	56 (50-61)	61 (55-65)	59 (54-65)
Sex			
Male N (%)	7 (58%)	17 (71%)	24 (67%)
Race			
Black N (%)	10 (83%)	6 (25%)	16 (44%)
White N (%)	2 (17%)	9 (38%)	11 (31%)
Hispanic/Latino** N (%)	0	2 (8%)	2 (6%)
American Indian N (%)	0	1 (4%)	1 (3%)
Declined/NA	0	6 (25%)	6 (17%)
Ethnicity			
Non-Hispanic N (%)	11 (92%)	13 (54%)	24 (67%)
Hispanic N (%)	1 (8%)	11 (46%)	12 (33%)
Duration of ART (months)			
Median (IQR)	162 (106-204)	136 (91-173)	144 (97-179)
Duration of viral suppression (months)			
Median (IQR)	69.5 (38-91)	79 (51-94)	75 (44-93)

*Percentage totals may not add up to 100 due to rounding. †IQR, interquartile range. **Participants may identify as Hispanic/Latino either in response to a question about their race, or a follow-up question on ethnicity. Participants who reported Hispanic ethnicity identified their race as either “White” or “Declined/Not Available.”

553 **Figure Legends**

554

555 **Figure 1.** HIV-1 reservoir size and intactness during opioid use. Quantifications were performed
556 on participants who used (n=24) or did not use (n=12) opioids. (a) HIV-1 persistence measures
557 in participants with (blue circles) and without (yellow circles) opioid use are shown. Data are
558 displayed on a logarithmic y-axis scale; DNA and RNA was extracted from 5 million PBMC.
559 Intact DNA was quantified with the IPDA assay. Mean values ± standard errors of the mean
560 (SEM) are shown. (b) 5' and 3' genomic deletions as a function of opioid use, mean values ±
561 95% CIs are displayed, (c) Opioid subgroup analysis. The reservoir size of intact, 5' deleted, and
562 3' deleted or hypermutated regions are shown. (d) The proportion of intact genomes as a function
563 of DNA copies and opioid use subgroup. Cohort 1, injection opioid use; cohort 2, prescribed oral
564 opioids for pain; cohort 3, methadone; cohort 4, suboxone; cohort 5, no opioid use.

565

566 **Figure 2.** HIV-1 latency reversal in OPHION participants. HIV-1 caRNA levels were quantified
567 after 24-hour incubations using 5 million PBMC and compared to a no-drug DMSO-containing
568 condition. Mean values and the 95% CIs are shown. (a) Combined data showing LRA responses
569 in thirty-six total participants with (blue circles) or without (yellow circles) opioid use. Data
570 from (a) was dichotomized by (b) opioid use, (c) sex (light purple circles, male; light grey
571 circles, female), and (d) race (light green circles, Black and American Indian; dark green circles,
572 white). (e) Opioid-use subgroup analysis highlighting LRA response to αCD3/αCD28 beads
573 from (a), as a function of opioid use subgroup. Means and SEM are shown. Dotted horizontal
574 line denotes a fold-change of 1. *$p<0.05$, ** $p<0.01$, *** $p<0.001$, and **** $p<0.0001$ for LRA
575 combinations, corrected for multiple comparisons. αCD3/αCD28, anti-CD3 anti-CD28

576 superparamagnetic beads; RMD, romidepsin; PNB, panobinostat; R, RMD 20nM; P, PNB
577 30nM; B, bryostatin 1nM; A, AZD5582 100nM.
578
579 **Figure 3.** Immune activation and cytokine induction during *ex vivo* LRA boosting. (a) Example
580 plots of $OX40^+PD\text{-}L1^+$, $OX40^+CD25^+$, and $CD69^+CD40L^+$ expression from live $CD4^+$ T cells in
581 PBMC samples incubated with DMSO control or an αCD3/αCD28 bead positive control for 18
582 hours, (b) Violin plots of surface activation-induced marker (AIM) response as a function of
583 LRA,. Results across three highly sensitive AIM assays for OPHION participants' samples
584 (n=36) are shown for comparison, (c) Quantification of LRA-induced surface CD69 expression
585 in live total $CD4^+$ T cells (n=36). Intracellular production of the cytokines TNF-α, IFN-γ, and IL-
586 2 during LRA exposure in (d) live $CD4^+$ and (e) $CD8^+$ T cells (n=36). Violin plot median values
587 are indicated by a solid black line; quartiles are shown with a dotted line. LRA conditions
588 without visible bars represent values < 0.1% of cells. *$p<0.05$, *** $p<0.001$, and **** $p<0.0001$
589 for LRA combinations, corrected for multiple comparisons. RMD, romidepsin; PNB,
590 panobinostat; R, RMD 20nM; P, PNB 30nM; B, bryostatin 1nM; A, AZD5582 100nM.
591
592 **Figure 4.** Histone H3 acetylation patterns during LRA exposure. (a) Violin plots showing the
593 proportion of live total $CD4^+$ T cells with acetylated histone H3, assessed by flow cytometry, (b)
594 Violin plot of mean fluorescence intensity (MFI) of acetylated histone H3 per live $CD4^+$ T cell.
595 Scatter plots of acetylated histone H3 levels per CD4 as a function of HIV-1 transcription in
596 response to (c) RMD and PNB monotherapy, (d) LRA boosting with HDACi and AZD5582, and
597 (e) HDACi in combination with low-dose bryostatin are shown. Acetylated histone levels and
598 HIV-1 reactivation with the combinations of HDACi and bryostatin were moderately positively

599 correlated (r=.25, p=.04). Violin plot median values are indicated by a solid black line; quartiles
600 are shown with a dotted line.
601
602 **Figure 5.** Comparative analysis of LRA boosting effects in PBMC and $CD4^+$ T cells.
603 Leukapheresis samples from HEAL cohort participants (n=11) were used to assess HIV-1
604 unspliced caRNA levels during (a) low-dose bryostatin-based and (b) AZD5582-based LRA
605 boosting combinations, when compared to PMA-ionomycin. Data are presented as means ±
606 SEM. Circle color is used to denote a given HEAL participant across Figure panels. (c) Absolute
607 HIV-1 unspliced caRNA levels in parallel PBMC and $CD4^+$ T cell LRA exposures. PBMC and
608 CD4 results are separated by a vertical dotted line. (d) Representation of the data in (c) as fold-
609 change in HIV-1 caRNA levels. (e) Corresponding HIV-1 RNA levels from culture supernatants.
610 (f) Multiply spliced HIV-1 RNA levels as determined in a modified TILDA assay, comparing
611 RMD-bryostatin combinations at two bryostatin concentrations to PMA-ionomycin. (g)
612 Combined OPHION and HEAL participant results (n=47) that summarize PBMC LRA boosting
613 responses, for LRA conditions common to both datasets. Results from OPHION participant
614 samples, carried over from Fig. 2a, are shown in grey circles. HEAL participant results are
615 shown in color. *p<0.05, ** p<0.01, *** p<0.001, **** p<0.0001, corrected for multiple
616 comparisons. NDC, no-drug control, contains 0.2% DMSO; PMAi, PMA with ionomycin; RMD,
617 romidepsin; PNB, panobinostat; R, RMD 20nM; P, PNB 30nM; B, bryostatin 1nM; A,
618 AZD5582 100nM.
619
620
621

Supplementary Figures Legends

Supplementary Figure 1. Substance use in the OPHION cohort. We assessed substance use by (a) clinical urine toxicology testing and (b) self-reported substance use questionnaires. Substance use results are separated by cohort groups by participant ID. Red squares indicate the presence of that substance in a urine sample; unavailable data were marked with "X" in a gray box. An expanded opiate panel was performed to assess for the presence of different opiate formulations. Color squares in panel b reflect any reported use by participants in the last 30 days. The numbers inside a given box indicate the number of days used this substance was reported to be used in the last 30 days. Gradient of color from blue to red indicate increasing report of use whereas white indicates no use. Concomitant use of alcohol, tobacco, marijuana, and gabapentin in the OPHION cohort was common. *all fentanyl measures were confirmed by follow-on quantification. Participants in the buprenorphine and methadone groups reported daily use of the respective medication in the 30 days prior, whereas participants taking opioids for chronic pain took opioids for 27-30 days in the 30 days preceding their enrollment in OPHION. 75% (N=3/4) of active injection users had urine toxicology screens positive for cocaine corresponding with self-report; all three reported smoking cocaine in the prior 30 days to specimen collection. One of twelve participants in the methadone use group and 2/12 in the non-opiate use group also has urine toxicology screens positive for cocaine. All active injection opioid users reported using multiple drugs on the same day in the last 30 days compared to 1/12 participants in non-opioid use group and 10/20 participants in methadone, buprenorphine and prescription opiate use groups combined. N=3/4 active injection opioid users reported smoking marijuana in the last 30 days. 6 and 8 participants about the 12 participants in opioid use groups had urine toxicology screens positive for benzodiazepines and gabapentin; all but 1 in both cases reported that this

substance was prescribed. No participant had urine toxicology screens positive for amphetamines or barbiturates. All participants injecting opioids used tobacco in the preceding 30 days and, overall, 23 of 36 OPHION participants used tobacco within the month prior to their blood collection. 25% (N=6/24) of opioid use participants consumed alcohol in last 30 days compared to 58% (7/12) in the control group.

Supplementary Figure 2. HIV-1 LRA boosting response in the OPHION cohort by ethnicity. HIV-1 fold-increase in unspliced RNA transcription plotted as a function of self-reported Hispanic (dark purple circles) or non-Hispanic (light blue circles) ethnicity.

Supplementary Figure 3. Flow cytometry gating strategies. Representative intracellular cytokine staining plots for (a) control and (b) αCD3/αCD28 bead-exposed PBMC are shown. (c) AIM assay and gating strategy and representative flow plots for control and αCD3/αCD28 bead-exposed PBMC.

Supplementary Figure 4. LRA-induced immune activation as a function of opioid use. Results obtained with the (a) OX40/PD-L1, (b) OX40/CD25, and (c) CD69/CD40L AIM assays are reported for all ten conditions in the LRA panel, where samples from participants with (blue circles) and without (yellow circles) opioid use are shown. Data are represented as means ± 95% CIs. The highest measured levels in OX40/PDL1 assay with bryostatin 1nM, R+B, and P+B are the same non-opioid-using participant. (d) Individual data points for $CD69^+$ live total $CD4^+$ T cells, as a function of opioid use. (e) Comparative hierarchies of intracellular cytokine production in $CD4^+$ and $CD8^+$ T cells exposed to αCD3/αCD28 beads. Data displayed in these

668 panels are identical to the data values shown in Main Fig. 3. *p<0.05, ** p<0.01, **** p<0.0001,
669 corrected for multiple comparisons. TNF, tumor necrosis factor-alpha; IFN, interferon-gamma;
670 IL-2, interleukin-2; CD4, $CD4^+$ T cells; CD8, $CD8^+$ T cells.
671
672 **Supplementary Figure 5.** Intracellular cytokine production, as a function of opioid use. Using
673 the same data displayed in Main Fig. 3, here we show individual data points, labelled as samples
674 from participants with (blue circles) and without (yellow circles) opioid use. $CD4^+$ T cell
675 production of (a) TNF-α, (b) IL-2, and (c) IFN-γ. CD8+ T cell production of (d) TNF-α, (e) IFN-
676 γ, (f) IL-2. No significant differences in cytokine production were observed by opioid use.
677
678 **Supplementary Figure 6.** Histone acetylation effects during LRA boosting, as a function of
679 opioid use. Using the same data displayed in Main Fig. 4, here we show individual data points,
680 labelled as samples from participants with (blue circles) and without (yellow circles) opioid use.
681 (a) The proportion of live total $CD4^+$ T cells with acetylated histone H3, assessed by flow
682 cytometry, (b) Mean fluorescence intensity (MFI) of acetylated histone H3 per live total $CD4^+$ T
683 cells.
684
685 **Supplementary Figure 7.** The effects of LRA boosting on human reference gene transcription.
686 Using leukapheresis samples from HEAL participants (n=9), we assessed and compared fold-
687 changes in transcription of three host genes: (a) IPO8, (b) TBP, and (c) UBE2D2. Reference
688 gene multiplexing was validated for (d) TBP and (e) UBE2D2 quantifications. The rationale to
689 study these three reference genes is as follows. IPO8 transcription is used as an internal control
690 by the AIDS Clinical Trials Group's Virology Specialty Laboratories to measure RNA integrity

in a dichotomous way. IPO8 Ct values >27 are used to suggest degradation of cellular samples in storage, and samples with IPO8 Ct >27 do not report HIV-1 RNA values. Recent work by Nancie Archin at the UNC HIV Cure Center identified TBP and UBE2D2 as two of the more stable host genes during LRA exposures, which included PMA, AZD5582, and HDACi, among a panel of eight LRA.

Supplementary Figure 8. Variance in LRA response. (a) Magnitude of HIV-1 caRNA transcription fold-changes in biological replicate LRA experiments performed with HEAL leukapheresis samples, derived from the data displayed in Main Fig 5a-c, (b) Box and whiskers plot displaying the data of Fig. 5g as the mean (solid black horizontal line), inter-quartile range (25^{th} – 75^{th} percentiles denoted as the borders of the vertical rectangle), and 5^{th}-95^{th} percentiles (whiskers, error bars). Values below and above the whiskers are shown as individual data points. PMA-iono, PMA with ionomycin; RMD, romidepsin; PNB, panobinostat; R, RMD 20nM; P, PNB 30nM; B, bryostatin 1nM; A, AZD5582 100nM.

Supplementary Tables

Supplementary Table 1 – Breakdown of OPHION cohort into opioid use subgroups

Supplementary Table 2 – HEAL Participant Characteristics

Online Methods

Study Design and Clinical Cohorts

The Opioids, HIV, and Translation (OPHION) study is a prospective cohort study of participants living with HIV on suppressive antiretroviral therapy recruited from Boston Medical Center which serves one of the largest populations of people living with HIV (PLWH) in Massachusetts, including a disproportionately large number of persons with opioid and substance use disorders. Eligible PLWH were required to currently be on antiretroviral therapy and virologically suppressed (defined as undetectable plasma HIV-1 RNA or <20 copies/ml) for a minimum of 12 months prior to enrollment. Individuals were recruited into 1 of 5 cohorts: (1) active injection opioid use, defined as self-report on injecting opioids at least once per week, (2) Methadone maintenance therapy for at least 3 months, (3) buprenorphine-naloxone therapy for at least 3 months, (4) Prescription oral opioid use for at least 6 months or (5) No opioid use within the past 1 year representing a control cohort. Eligibility into each of the five cohorts was confirmed with a urine toxicology performed at the BMC central laboratory, which includes evaluation for urine drug metabolites including opiates and non-opioid substances as well as an expanded opioid panel which included fentanyl or norfentanyl metabolites. Exclusionary criteria included ongoing immunosuppression and pregnancy; patients who reported injecting non-opioid substances were also not eligible. Once consented and enrolled, each participant underwent blood collection for same day PBMC extraction as well as urine collection for gabapentin and benzodiazepine metabolites. Participants also completed an extensive survey on their current and prior substance use (including alcohol and tobacco use) based the addiction severity index (ASI) [63] and Texas Christian University (TCU) drug screen [64]. HIV and other clinical information including ART

736 treatment history, duration of virologic suppression and comorbidity status including hepatitis C
737 and B were abstracted from the medical record.

738 The HIV Eradication and Latency (HEAL) Cohort is a longitudinal biorepository study of
739 participants with HIV. Inclusion criteria for HEAL participants in this study were 1) ART-treated
740 participants with HIV-1 who were virologically suppressed, defined as plasma HIV-1 RNA less
741 than assay (most commonly less than 20 copies/mL, without blips) for >1 year and 2) had
742 sufficient available amounts of cryopreserved PBMC for the proposed analyses. These cohort
743 studies are performed in accordance with the principles of the Declaration of Helsinki. The
744 institutional review boards at Boston Medical Center and Brigham and Women's Hospital (Mass
745 General Brigham Human Research Committee) approved the study protocols. Written informed
746 consent was obtained from all participants. Experimenters were blinded to all clinical data and to
747 OPHION subgroup assignments.

748

749 **Quantification of HIV-1 persistence markers**

750 Genomic DNA and total RNA were isolated from approximately $5x10^6$ peripheral blood
751 mononuclear cells (PBMC) or total $CD4^+$ T cells (AllPrep DNA/RNA kit, Qiagen). Total HIV-1
752 DNA and unspliced cell-associated RNA (caRNA) levels were quantified in triplicate by real-
753 time PCR as previously described, modified to include Taqman Universal Mastermix (DNA) or
754 Taqman Fast Virus 1-Step Mastermix (RNA) [65]. HIV-1 quantifications used forward primer 5'-
755 TACTGACGCTCTCGCACC-3', reverse primer 5'-TCTCGACGCAGGACTCG-3', and probe
756 5' FAM-CTCTCTCCTTCTAGCCTC-MGB 3' (ThermoFisher Scientific). DNA cycling
757 conditions in a total reaction volume of 25µL were 95°C for 15 min followed by 40 cycles of
758 95°C for 15 sec and 60°C for 1 min. RNA cycling conditions in a total reaction volume of 20µL

were 55°C for 15 min, 95°C for 20 sec, followed by 40 cycles of 95°C for 3 sec and 60°C for 30 sec. Approximately 500ng of genomic DNA were assessed per well. The limits of quantification for total HIV-1 DNA and unspliced caRNA were 1 and 3 copies per reaction, respectively. Limits of detection were calculated per timepoint and participant sample, considering the average number of copies detected across triplicate measurements. Cell input numbers were quantified by human genome equivalents of CCR5 DNA using forward primer 5'-ATGATTCCTGGGAGAGACGC-3', reverse primer 5'-AGCCAGGACGGTCACCTT-3', and probe 5' FAM-CTCTCTCCTTCTAGCCTC-MGB 3' (ThermoFisher Scientific) as described [65].

Intact proviral DNA assay

HIV-1 DNA from isolated PBMC DNA was measured using the intact proviral DNA assay (IPDA) [66]. Briefly, a multiplex droplet digital PCR assay was performed using primer and probe sets targeting the Psi packaging signal and env regions of the HIV-1 genome using 700 ng DNA per well. Intact provirus genomes were indicated in double positive droplets whereas incomplete genomes were single positive and classified as either 5' (Psi-/env+) or 3' (Psi+/env-) deletions. Quantified proviral sequences were normalized to cell number reference gene RPP30 and expressed as copies per million PBMC. Data was generated using the Bio-Rad QX200 Droplet Digital PCR system and analyzed using QuantaSoft Data Analysis Software.

Multiply spliced HIV-1 transcripts

To measure the frequency of total $CD4^+$ T cells with inducible multiply spliced HIV-1 RNA, we performed the TILDA assay, as previously described, with two modifications [46]. First, to reduce the 95% CIs around our frequency estimates, we used 36 x 10^6 cells/mL as our first dilution,

782 rather than the 18 x 10^6 cells/mL used in Procopio, et al. Second, to harmonize our PMA-
783 ionomycin concentrations with LRA experiments, we reduced the PMA concentration from its
784 original 100 ng/mL to 50ng/mL in our TILDA assays. The duration of virologic suppression in
785 our HEAL participants was similar to previously reported participants [46].
786
787 **Reference gene quantification**
788 Extracted PBMC RNA was used to quantify transcription levels of three host genes, IPO8, TBP,
789 and UBE2D2, typically immediately after the loading of HIV-1 caRNA qPCR plates was
790 complete. IPO8 quantifications used forward primer 5'- CCTTTGTACAACAGAAGGCAC -3',
791 reverse primer 5'- TGCACGTCTCAGGTTTTTGC -3', and probe 5' FAM-
792 TCCGCATAAATCCATTGATTCTGC -MGB 3' (ThermoFisher Scientific); TBP
793 quantifications used forward primer 5'- CAGTGAATCTTGGTTGTAAACTTGA -3', reverse
794 primer 5'- TCGTGGCTCTCTTATCCTCAT -3', and probe 5' FAM-
795 CGCAGCAAACCGCTTGGGATTAT -MGB 3' (ThermoFisher Scientific); and UBE2D2
796 quantifications used forward primer 5'- GTACTCTTGTCCATCTGTTCTCTG -3', reverse
797 primer 5'- CCATTCCCGAGCTATTCTGTT -3', and probe 5' VIC-
798 CCGAGCAATCTCAGGCACTAAAGGA -MGB 3' (ThermoFisher Scientific). To generate
799 IPO8 standards, we cloned a fragment corresponding to nucleotides 3636-3707 of IPO8 mRNA
800 (Sequence ID NM_006390.4) into a pCR4-TOPO vector (ThermoFisher Scientific, Cat. No.
801 K458001). To generate TBP standards, a fragment corresponding to nucleotides 649-1037 of
802 TBP mRNA (Sequence ID NM_003194) was cloned into a pCR4-TOPO vector. To generate
803 UBE2D2 standards, a fragment corresponding to nucleotides 729-1164 of UBE2D2 mRNA
804 (Sequence ID NM_181838.2) was cloned into a pCR4-TOPO vector. Reference gene RNA was

805 synthesized using T3 Megascript Kit (ThermoFisher Cat. No. AM1333 and cleaned (RNease
806 MinElute Cleanup Kit, Qiagen, Cat. No. 74204) before serially diluting across a range of 10^6 –
807 10^3 copies per well. After TBP and UBE2D2 standards were individually validated, TBP (T)
808 and UBE2D2 (U) RNA were diluted separately and aliquoted together as one set of multiplex
809 standards. T and U standards were validated to demonstrate overlap of individual and
810 multiplexed standards curves. The assay was optimized to run all host gene standards and
811 samples on one 96-well reaction plate in a total reaction volume of 20µL using cycling
812 conditions of 55°C for 5 min, 95°C for 20 sec, followed by 40 cycles of 95°C for 3 sec and 56°C
813 for 30 sec. Reference gene standards and samples were run in duplicate. IPO8, TBP, and
814 UBE2D2 RNA copies per million PBMC were calculated by dividing copies per total sample by
815 number of cells per sample, determined by CCR5 quantification, and normalized to $1x10^6$ cells.
816 Fold changes were calculated by dividing the RNA copy number obtained per million PBMC for
817 each LRA condition by the 0.2% DMSO control condition's reference gene RNA copies/million
818 PBMC.
819
820 **HIV-1 latency reversal**
821 OPHION and HEAL participant peripheral blood mononuclear cells (PBMC) were isolated from
822 large volume (90 – 180cc) peripheral blood or leukapheresis collections by density centrifugation
823 and cryopreserved. Cryopreserved PBMC were thawed, pelleted, and transferred to RPMI media
824 supplemented with 10% fetal bovine serum, 2 µM raltegravir, and 2 µM tenofovir (R10 +
825 TDF/RAL) at a concentration of $1x10^6$ cells/mL. Cells were rested in a humidified CO_2
826 incubator at 37°C for three hours (hrs). After 3hrs, cells were counted and assessed for viability.
827 For $CD4^+$ T cell experiments, PBMC were pelleted, resuspended in EasySep Buffer (StemCell

Technologies, cat. no. 20144), and isolated with EasySep Human $CD4^+$ T Cell Enrichment Kit (StemCell cat. no. 19052) per the manufacturer's instructions. A total of $5x10^6$ PBMC, or total $CD4^+$ T cells, were aliquoted into 5mL of fresh R10 + RAL/TDF in 6-well sterile cell culture plates. Cells were incubated in the presence or absence of the following LRA conditions: 0.2% DMSO, 1:1 αCD3/αCD28 beads (Life Technologies, cat. no. 11131D) to cells with 30 U/mL IL-2 (R&D Systems, cat. no. 202-IL-500), romidepsin 20 nM (Sigma , cat. no. SML1175), panobinostat 30nM (Sigma, cat. no. SML3060), bryostatin-1 1nM (Sigma, cat. no. B7431), AZD5582 100nM (ChemieTek, cat. no. CT-A5582), romidepsin 20 nM plus bryostatin-1 1nM, panobinostat 30nM plus bryostatin-1 1nM 100nM, romidepsin 20 nM plus AZD5582 100nM, panobinostat 30nM plus AZD5582 100nM, and phorbol 12-myristate 13-acetate (PMA) 50ng/mL (Sigma, cat. no. P1585) in combination with ionomycin 1μM (Sigma, cat. no. I9657). To provide a known positive control for subsequent immunology assessments, αCD3/αCD28 beads were used with OPHION samples. Cultures were incubated at 37°C for 24 hours. After 24 hours, cells were prepared for nucleic acid extractions.

Activation Induced Marker (AIM) assay

AIM assays were performed as previously described [43]. Briefly, cryopreserved PBMC were thawed, washed, resuspended in R10, and rested for 3 hours at 37°C. Following the 3-hour rest interval, the appropriate number of cells were transferred to a 48-well plate and subsequently treated with CD40 blocking antibody (Miltenyi Biotec, cat. no. 130-094-133) for a final concentration of 0.5ug/mL for 15 minutes at 37°C. Cells were incubated in the presence or absence of our 10-LRA panel, as previously described. After an 18hr incubation, cells were harvested and stained for 50 minutes at 4°C with the surface staining monoclonal antibodies

(mAb); (PD-L1-PE/Cy7 (Biolegend, cat. no. 329717), CD40L-PE (BD Biosciences [BD], cat. no. 561720), OX40-APC (BD cat. no. 563473), CD69-BV650 (Biolegend cat. no. 310933), CD3-BV605 (Biolegend cat. no. 317322), CD4-BV421 (BD cat. no. 562424), CD8-PerCp-Cy5.5 (BD cat. no. 560662), CD25- BUV395 (BD cat. no. 564034) and LIVE/DEAD Near-IR stain (ThermoFisher cat. no. L34975), washed, fixed and permeabilized (BD cytofix fixation buffer, cat. no. 554655), and then stained for 30 minutes at 4°C with intracellular mAb Acetyl-histone H3-Alexa Fluor 488 (Cell Signaling Technology, cat. no. 9683S) in 1x perm/wash buffer (BD, cat. no. 554723). The cells were washed and fixed (BD cytofix fixation buffer, cat. no. 554655) prior to flow cytometry analysis.

Intracellular cytokine staining

Cryopreserved PBMC were thawed, washed, resuspended in RPMI + 10% FBS (R10), and rested for 3 hours at 37°C. Following the 3-hour rest interval, the appropriate number of cells were transferred to a 48-well plate and incubated for 2 hrs with our panel of 10 LRA. Following this 2-hour incubation period, GolgiPlug (BD, cat. no. 555029) and GolgiStop (BD, cat. no. 554724) were added to each condition at a concentration of 1:1000 and 6:10000 respectively, then incubated at 37°C for an additional 16 hrs. Cells were harvested, pelleted, resuspended, stained for 20 minutes at 4°C with surface staining mAb (CD3-BV605, CD4-BV421, CD8-PerCp-Cy5.5 and LIVE/DEAD Near-IR stain), fixed and permeabilized as described above, and then stained for 30 minutes at 4°C with the intracellular mAb TNF-α- PE/Dazzle-594 (Biolegend cat. no. 502946), IL-2- PE/Cy7 (BD cat. no. 560707) and IFN-γ- BV510 (Biolegend cat. no. 502544). PBMC were washed and fixed in (BD cytofix fixation buffer, cat. no. 554655) prior to flow cytometry analysis, as described above.

874

875 **Flow cytometry**

876 Cells were acquired on a BD LSRFortessa using FACSDiva. Analysis was performed using
877 FlowJo software versions 10.6.2 (Treestar, Versions 10 for Mac). Representative gating
878 strategies can be found in the supplemental figures.

879

880 **Statistical analysis**

881 Statistical analyses were performed using GraphPad Prism 9 for macOS. Means, medians, 95%
882 confidence intervals, and standard errors of the mean were calculated. The pre-specified primary
883 outcome of OPHION was a comparison of $\log_{10}$ PBMC HIV-1 caRNA levels between
884 participants who use and do not use opioids. The pre-specified outcome for OPHION latency
885 reversal experiments was the difference in HIV-1 caRNA levels between LRA treatment groups
886 and across opioid use groups. To assess for changes in HIV-1 caRNA, we performed Kruskal-
887 Wallis testing of all participants together for each of the LRAs with Dunn's multiple comparison
888 test, comparing the mean rank of each LRA condition with the mean rank of every other LRA
889 condition. An identical approach was taken with a series of exploratory analyses with OPHION
890 participant samples that assessed histone acetylation, surface activation, and intracellular
891 cytokine production, and with the exploratory statistical analyses performed on experiments with
892 HEAL participant samples.

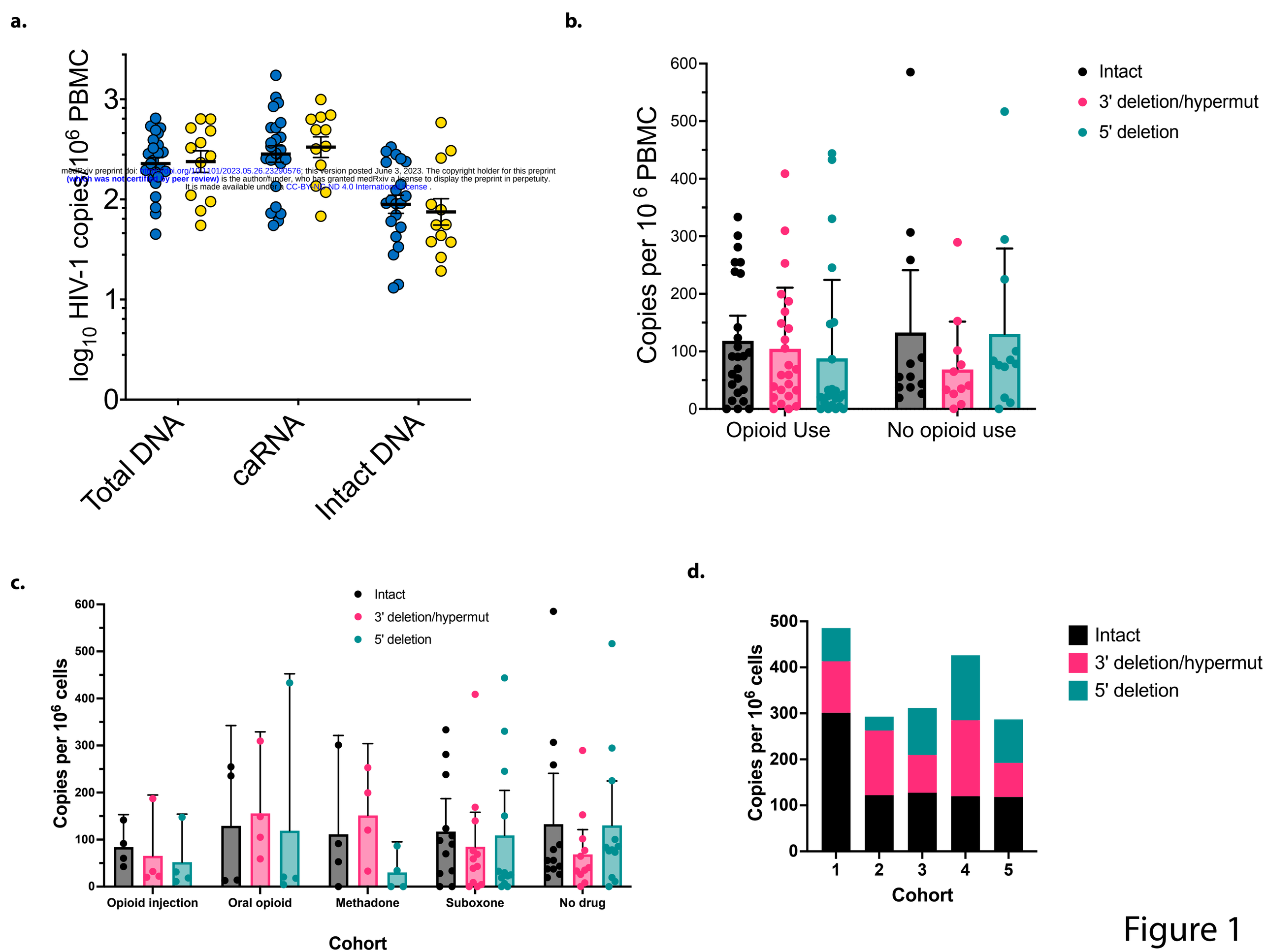

Figure 1

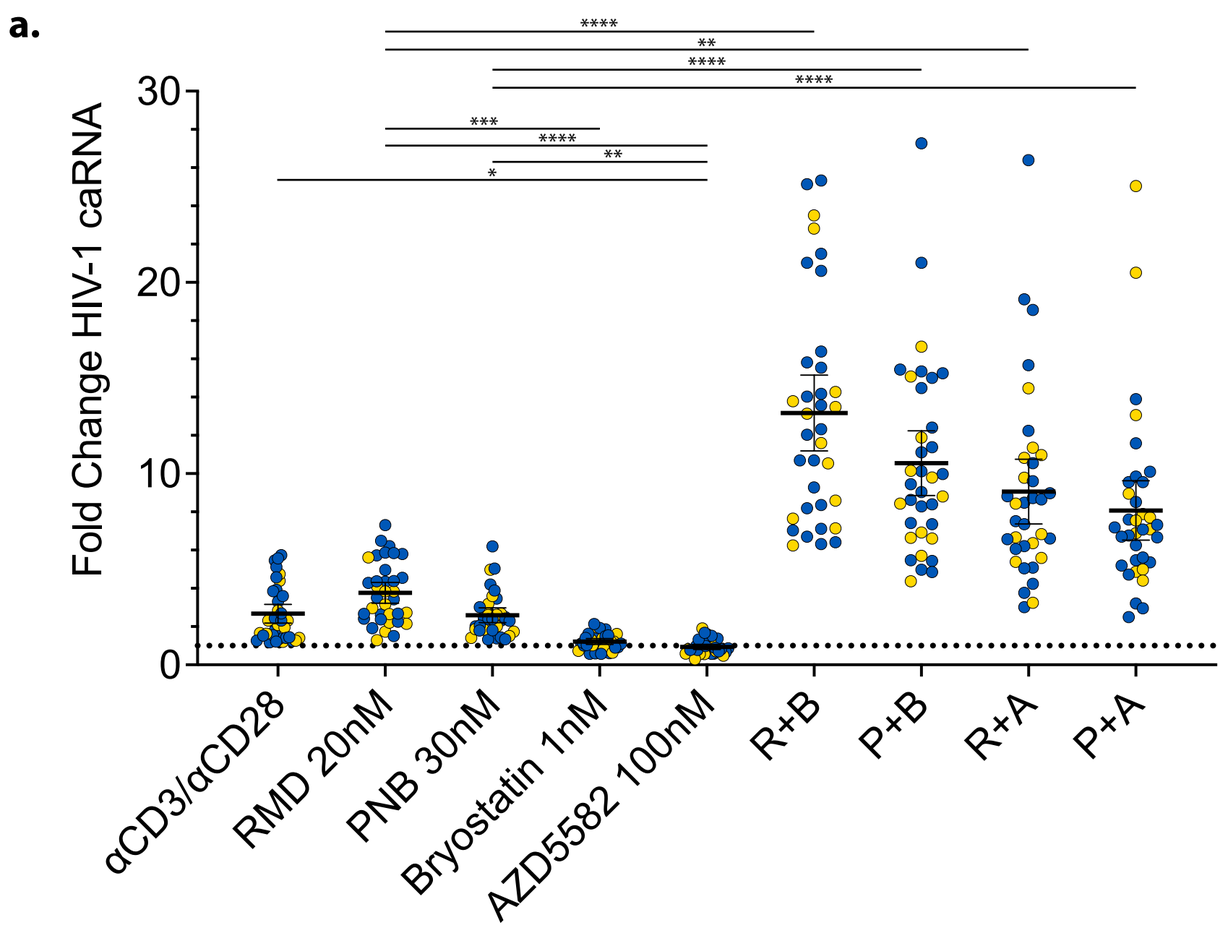

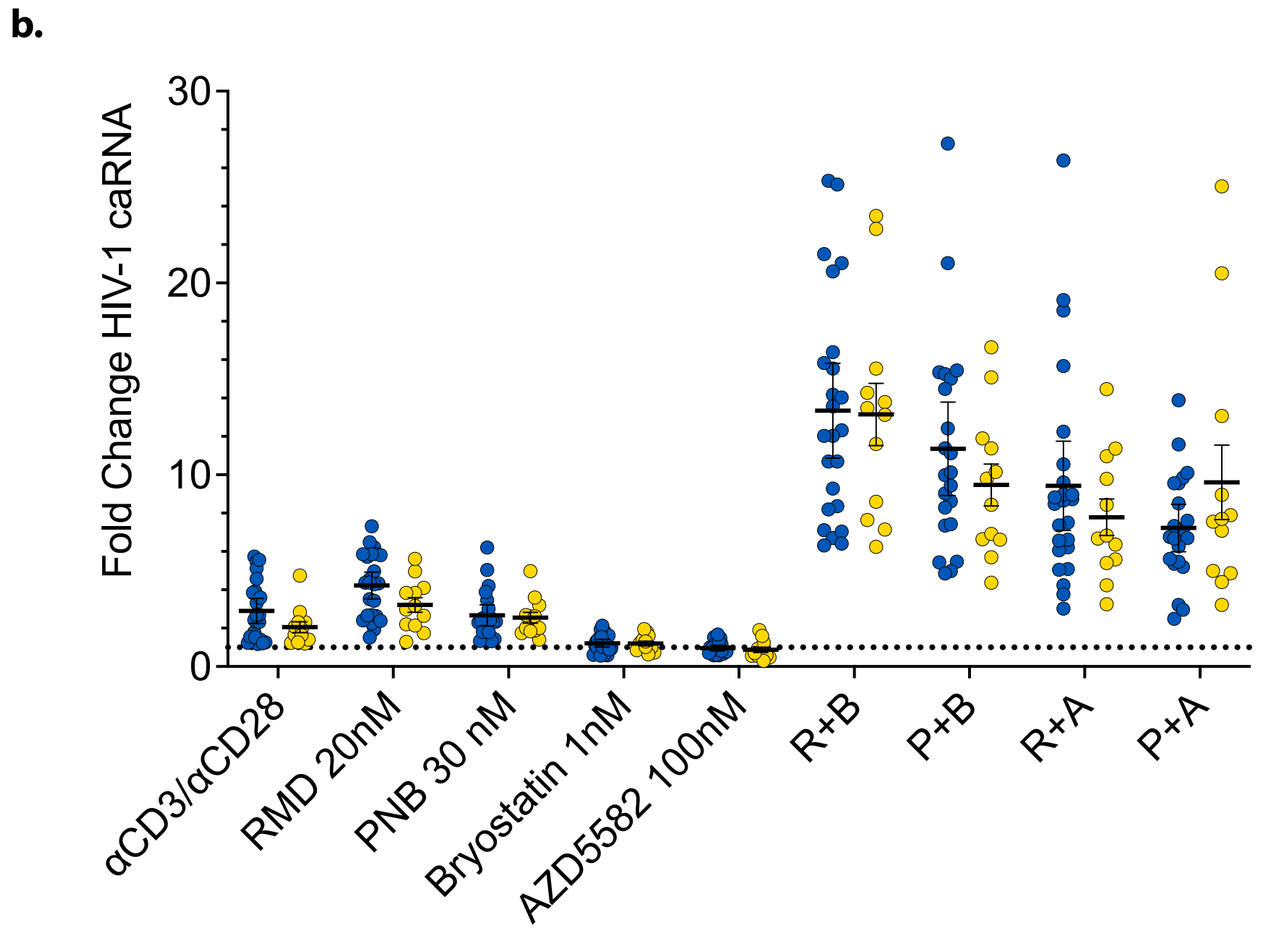

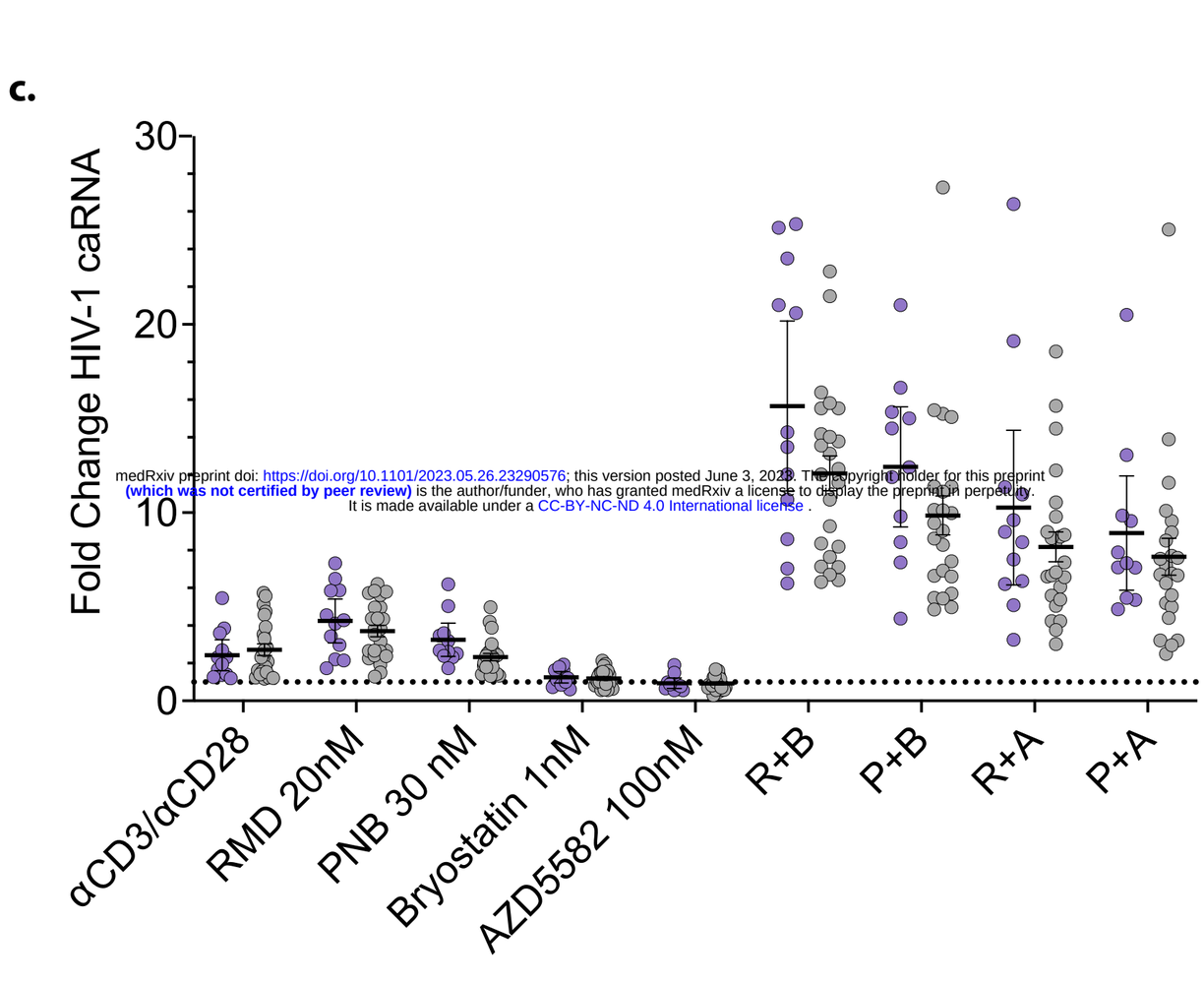

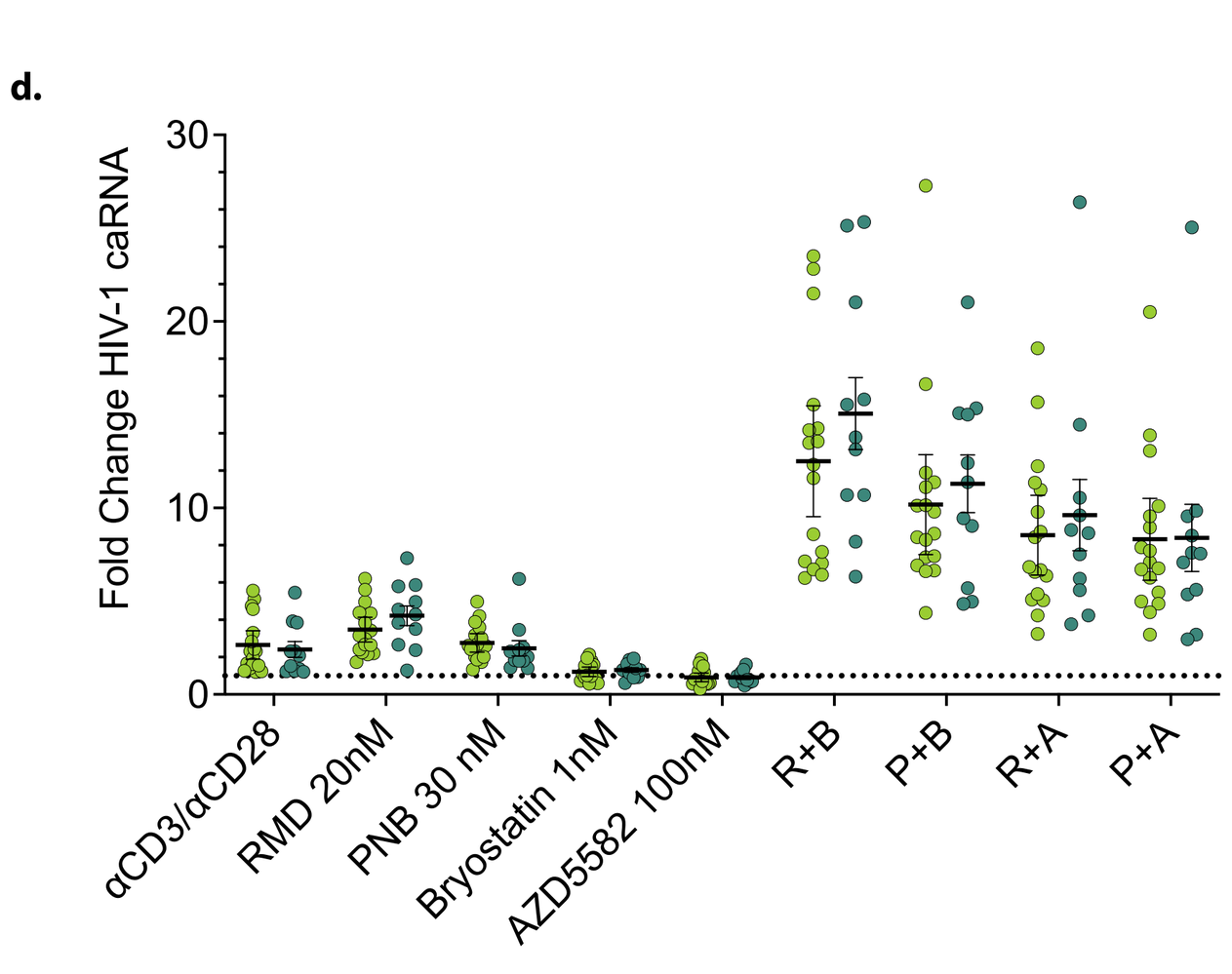

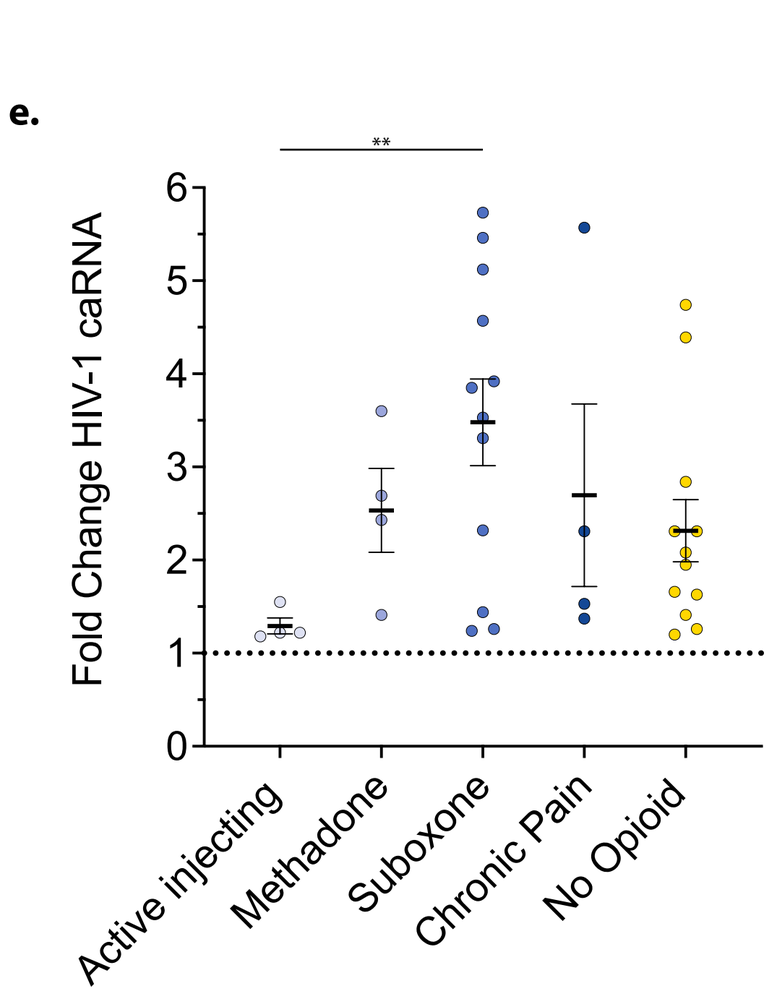

Figure 2

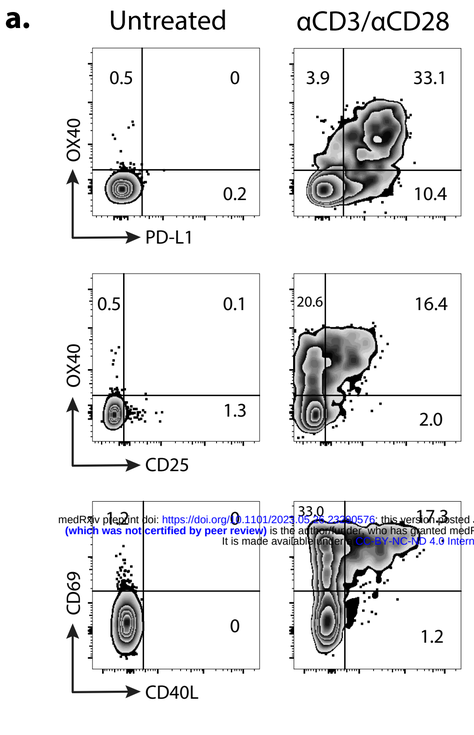

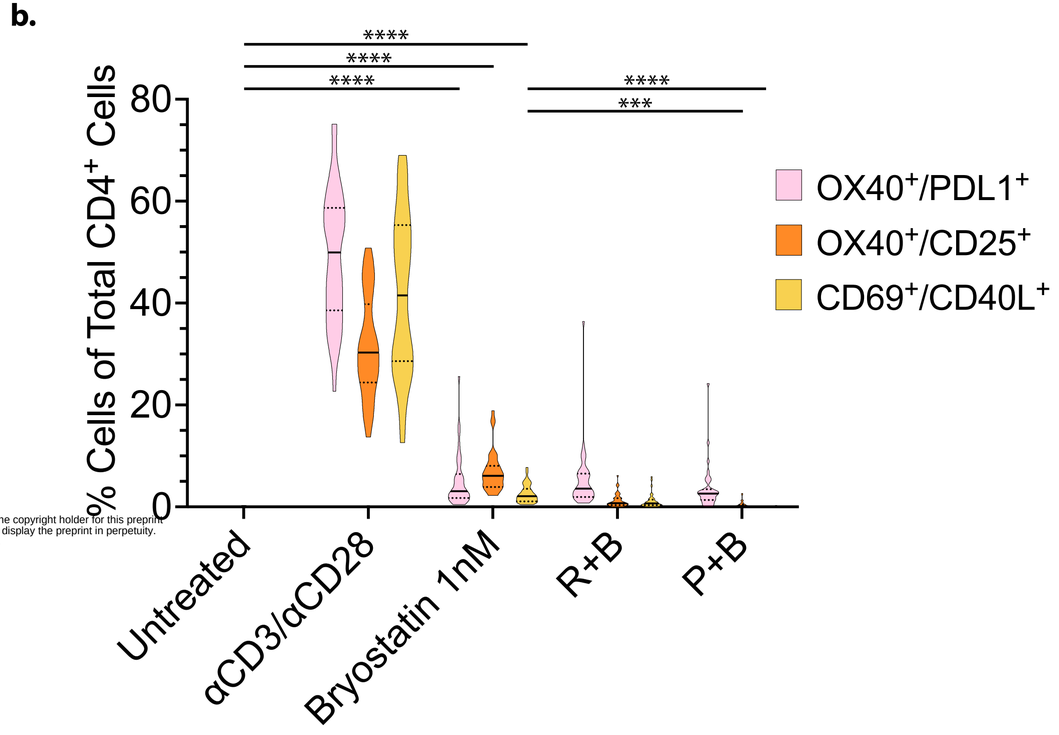

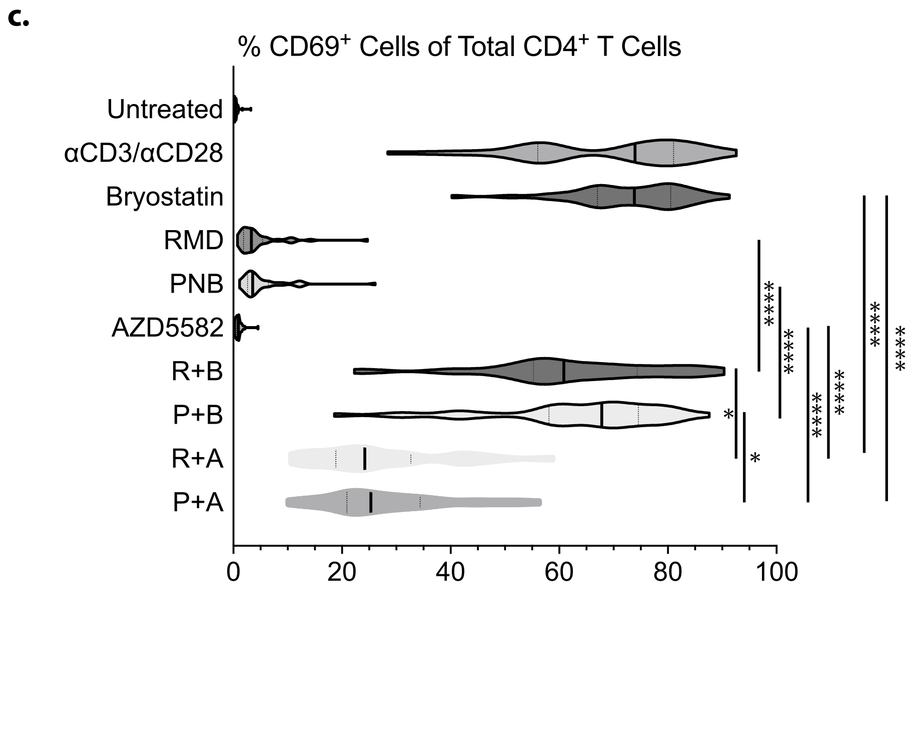

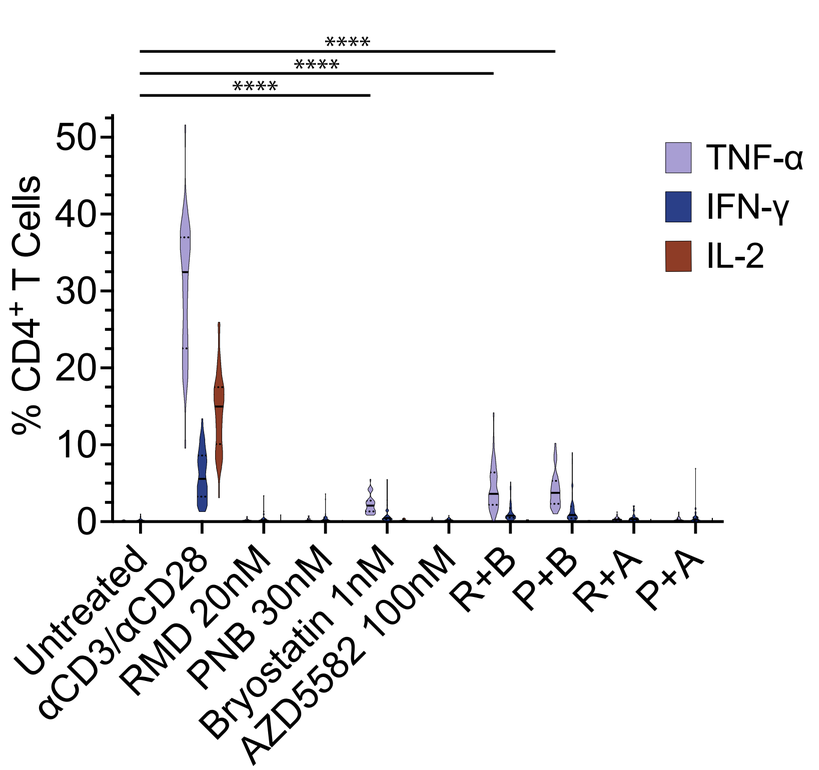

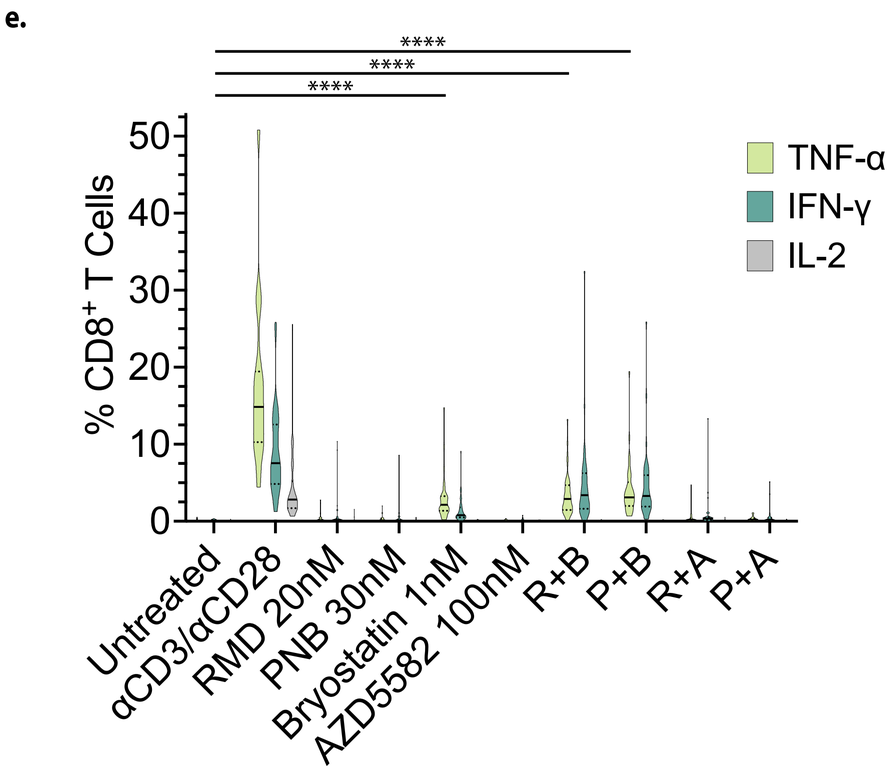

Figure 3

Figure 4

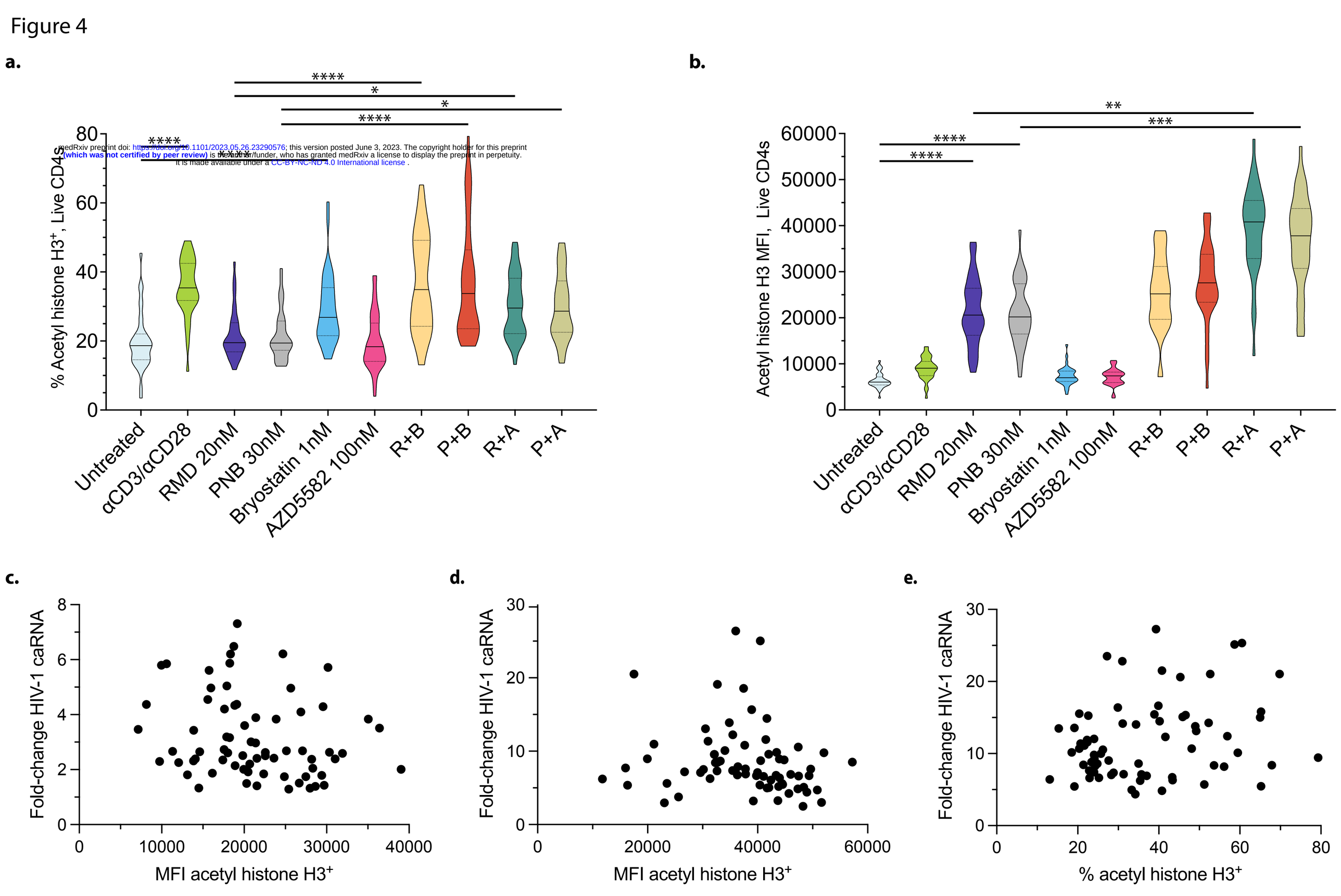

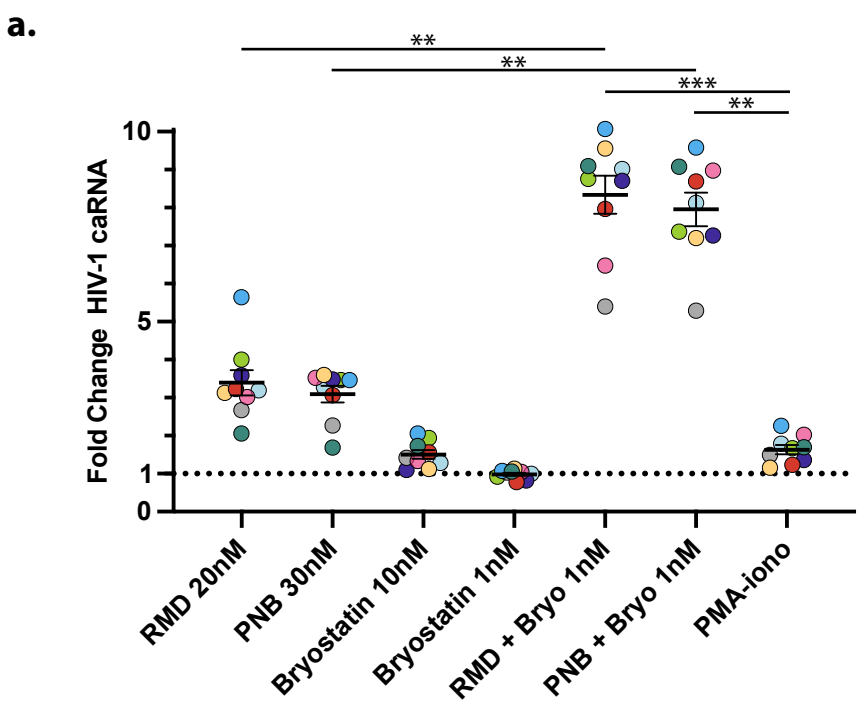

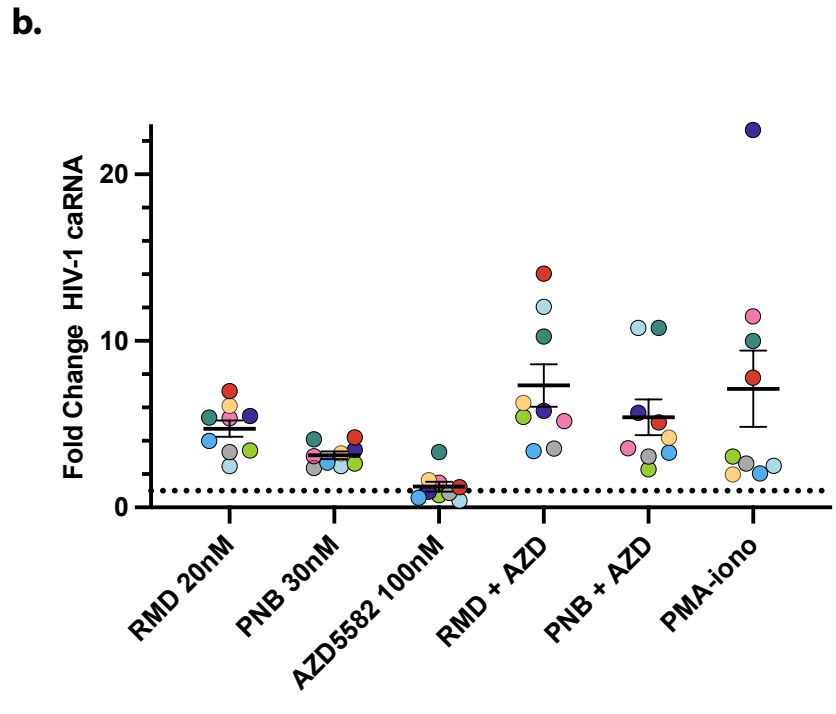

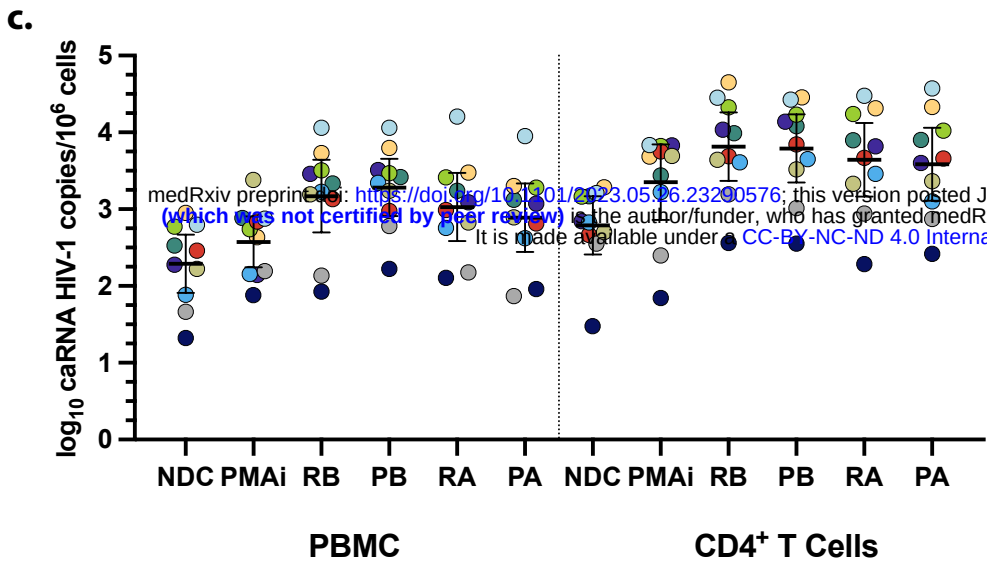

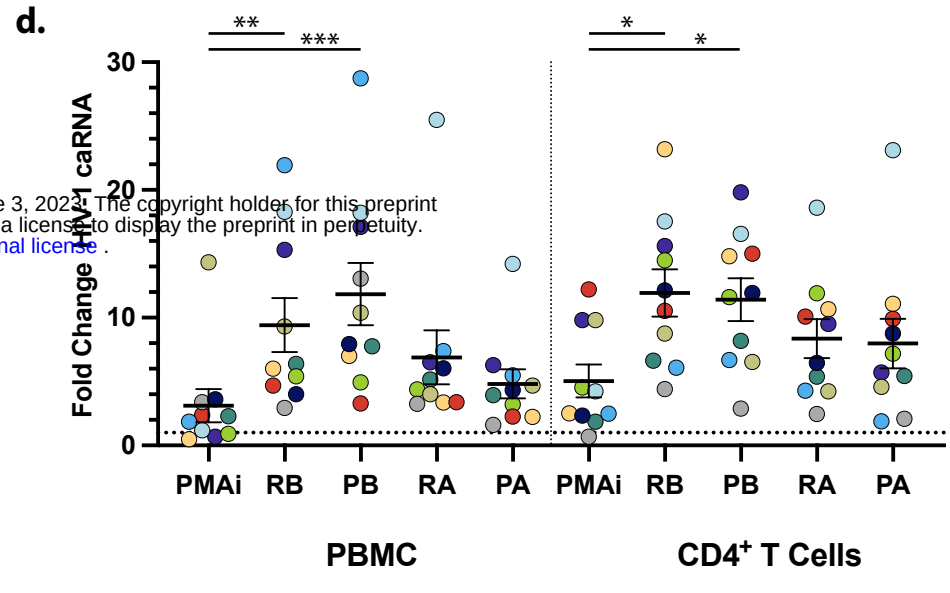

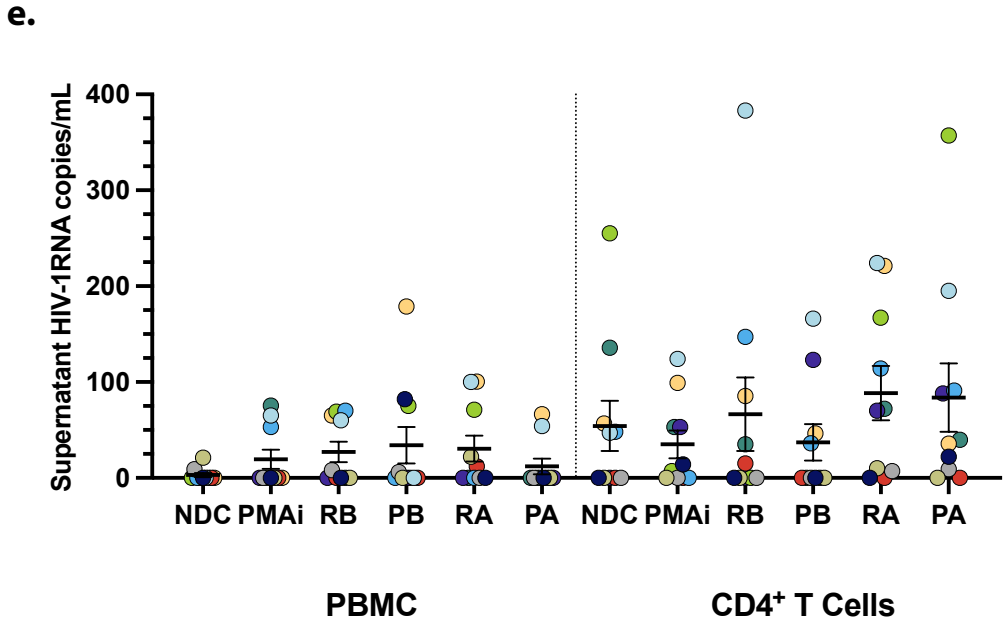

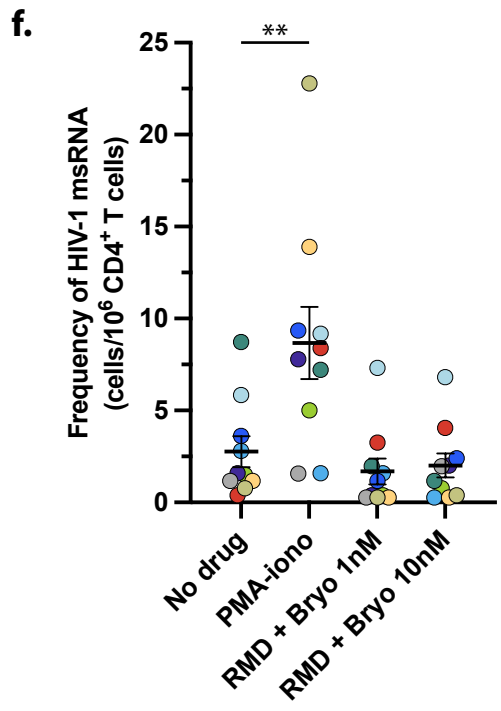

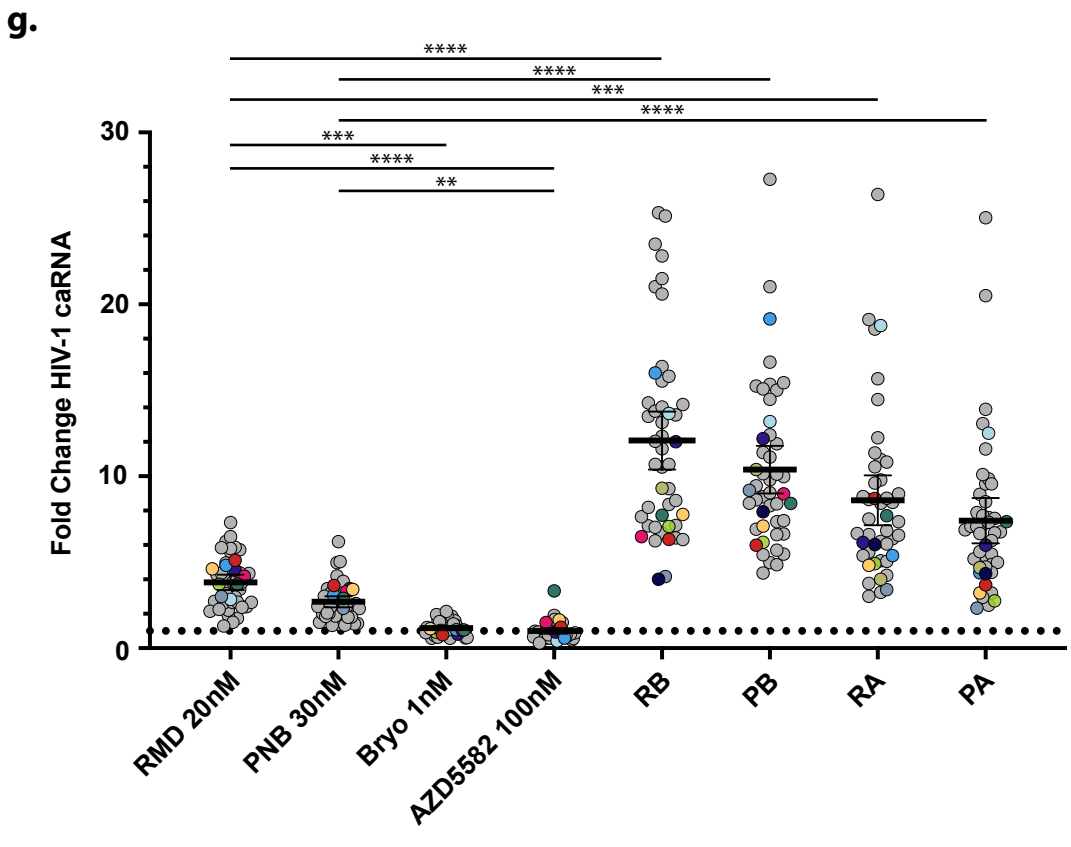

Figure 5